

Beacons in the sky help monitor Earth's orientation in space



Measurements of remote celestial objects detail Earth's orientation in space.

By Laura Naranjo

Illustrations of Earth depict a circular planet, steadily rotating on its axis orbiting the sun. Reality is not so tidy. Earth is not perfectly round; it wobbles, spinning at a slightly irregular rate. Geodesists, researchers who study Earth's shape, movement, and orientation in space, help us get where we want. Accurately accounting for an imperfect Earth means the next time you use GPS, you will locate the correct restaurant or find your way out of a remote canyon.

- [About the data](#)
- [About CDDIS](#)

Maintaining such precision requires continuous effort. To keep up with Earth's constant change, from its rotation to its tectonic movement, researchers have created terrestrial and celestial frameworks of carefully observed reference points to triangulate positions accurately. These points help form reference frames that go beyond locating Earth in space, they reveal Earth's tiny shifts caused by earthquakes and land rebounds after ice sheets melt. Such minute changes can only be observed if Earth's motion is precisely measured.

From radio waves to reference frames

These reference frames are based on two sources near and far: radio telescopes on Earth, and the extremely distant celestial objects they detect.

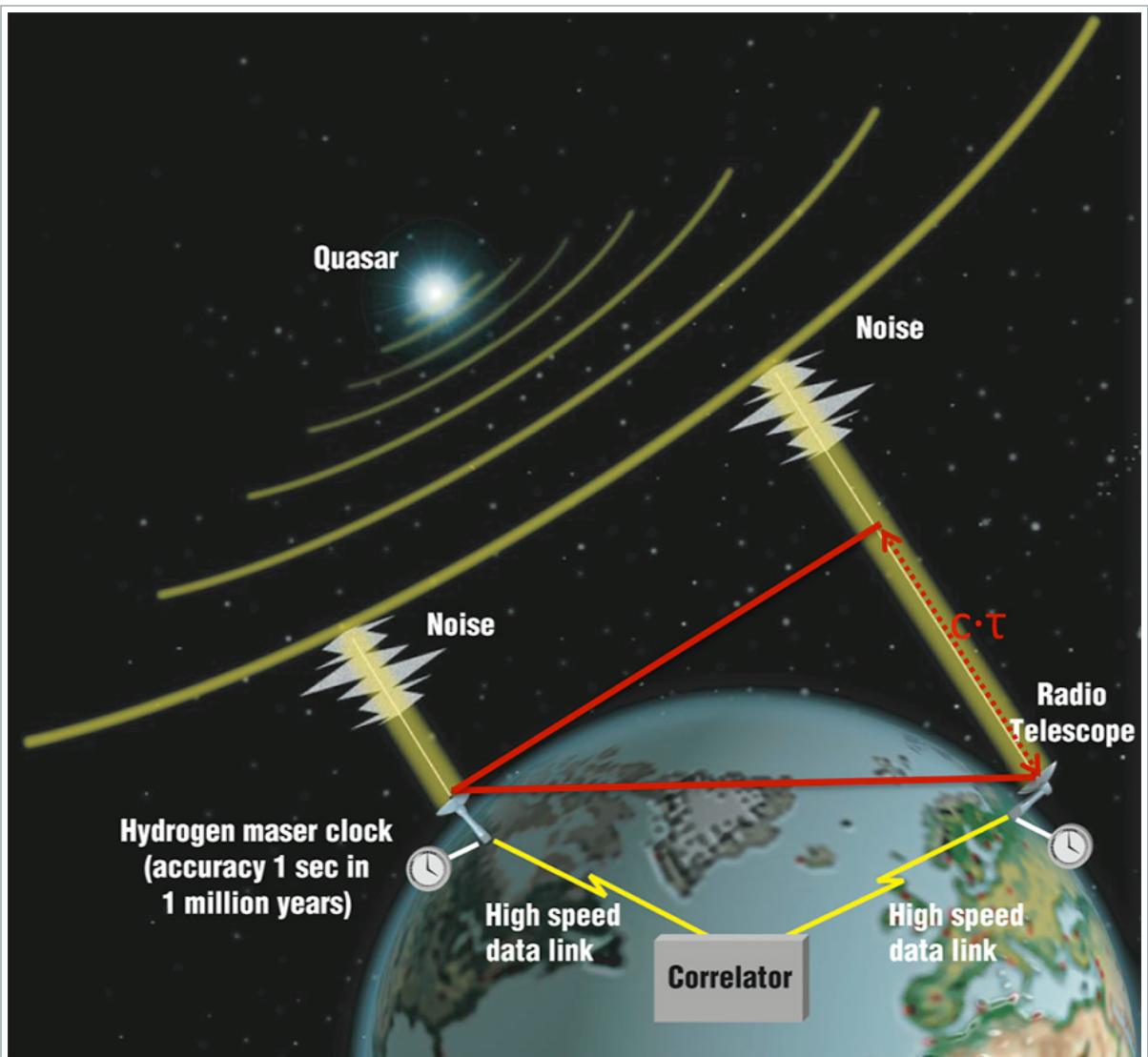
In the 1930s, engineer Karl Jansky discovered that celestial objects emit radio waves when he tried to locate radio interference. Using a large antenna, he determined Earthly sources of radio waves, yet remained puzzled by unidentified sources. After comparing the signal to astronomical charts, Jansky realized the radio waves were "star noise," coming from the constellation of Sagittarius - 25,640 light years away from Earth.



These radio telescopes at Geodetic Observatory Wettzell in Germany are part of the International Very Long Baseline Interferometry (VLBI) Service for Geodesy and Astrometry (IVS). (Courtesy Uwe Hessels)

Following Jansky's discovery, researchers raced to build dish-shaped radio telescopes. Unlike tubular optical telescopes, radio telescopes cradle an antenna in a large parabolic dish, designed to channel radio waves from very specific directions—a distant galaxy, for instance. The first dish measured only 9 meters (30 feet) across. To detect more distant celestial objects, however, dishes needed to be much larger. Many radio telescope dishes are now 25 to 100 meters (82 to 328 feet) across. "The larger dishes are more sensitive, and used more for the faint sources," said NASA geodesist Dirk Behrend. Now hundreds of radio telescopes across Earth's surface tilt skyward, capturing a continuous stream of radio waves.

Size was not enough, however. More powerful radio telescopes were required to study extremely remote celestial objects in greater detail. So in the 1960s, researchers developed a technique called Very Long Baseline Interferometry (VLBI) to increase resolution. "VLBI is a technique where you combine the signals from multiple radio telescopes to synthesize a much larger radio telescope," said David Gordon a radio astronomer at NASA's Goddard Space Flight Center. As radio waves from distant objects arrive, there is a time delay in a particular part of the signal arriving at one antenna versus another antenna. In that tiny delay, researchers extract a world of data. "We can measure the separation between the antennas, the rotation of the Earth, the polar motion of the Earth, the nutation, and the source coordinates," Gordon said.



Very Long Baseline Interferometry combines the signals from two or more radio telescopes to synthesize a much larger radio telescope. As radio waves from distant objects arrive, there is a delay in the time the signal arrives at one antenna versus another antenna. The VLBI technique uses the tiny time difference to help observe the object's structure and location. (Courtesy NASA)

This technique permitted astronomers to study more compact celestial objects and phenomena. Through painstaking observations, researchers precisely locate cosmic sources to develop what is called the International Celestial Reference Frame (ICRF). Behrend said, "The celestial frame is based on extremely distant extra-galactic radio sources called quasars; these are remote objects, typically brighter than a billion suns, which are embedded in the center of galaxies." Quasars are so remote that they appear fixed, making them good reference sources. "The stars around us show motion over a few years," Gordon said. "But quasars should essentially be fixed for much longer periods of time, perhaps thousands of years."

Researchers also use the VLBI time delays from distant fixed objects to measure ground motion underneath radio telescope sites. Continental drift causes extremely slow changes, only a few centimeters per year, or about the rate that fingernails grow. Earthquakes, however, can cause sudden changes. Precisely measuring the position of each VLBI telescope site helped develop a set of Earth-based coordinates and velocities, contributing to a terrestrial reference frame representing measurements taken at a particular point in time. In addition to VLBI telescopes, this terrestrial framework includes three other space-geodetic techniques and their instruments: Satellite Laser Ranging (SLR) telescopes, Global Navigation Satellite Systems (GNSS) antennas, and Doppler Orbitography by Radiopositioning Integrated on Satellite (DORIS) beacons.

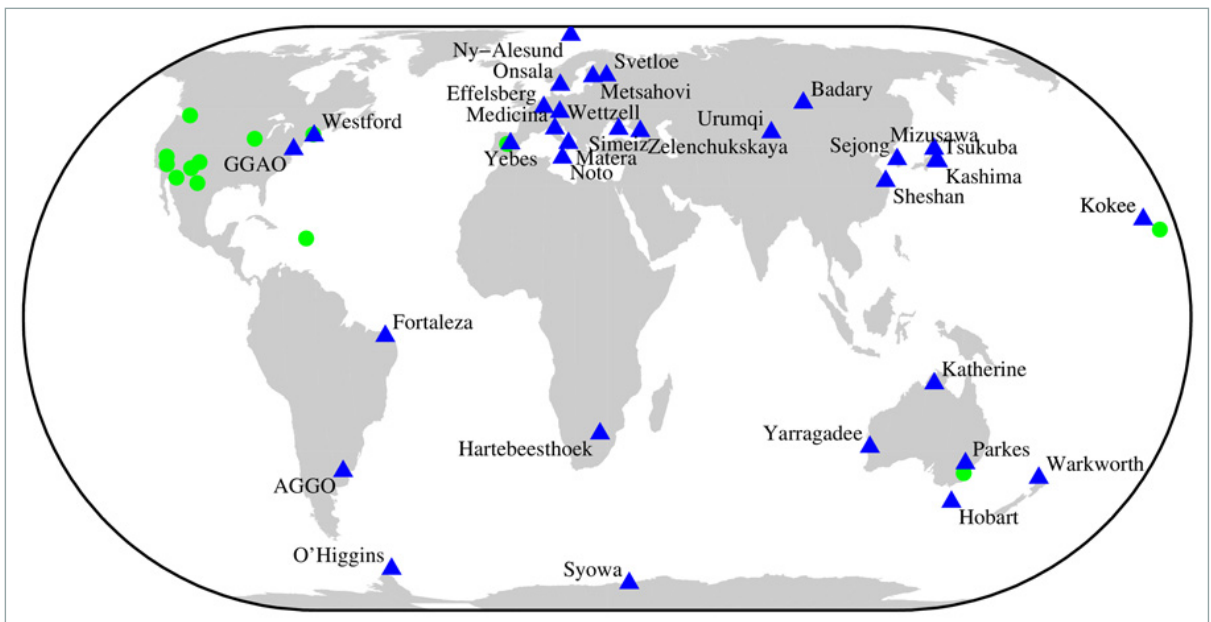
VLBI bridges the terrestrial and celestial reference frames. The telescope sites form part of the terrestrial reference frame on a constantly rotating and shifting Earth, while quasars detected by the VLBI technique help form the fixed

celestial reference frame. "By observing quasars all around the sky and measuring the delays for each one of them on each baseline, you can use a method of triangulation to solve for where the quasar is, where the Earth is, what the Earth orientation is," Gordon said.

Earth Orientation Parameters

In the 1970s, NASA helped develop VLBI because accurate and repeated observations could discern motion in Earth's crust. By 1979, NASA had established the Crustal Dynamics Project (CDP) at Goddard, and created NASA's Crustal Dynamics Data and Information Service (CDDIS) to archive and distribute CDP data. Early achievements of VLBI include measuring the rate of tectonic spreading between North America and Europe, as well as tracking tectonic deformation along the San Andreas fault in the southwestern US. The VLBI technique has also measured earthquake motion in Alaska, California, Hawaii, Chile, and Japan. Researchers continue to rely on VLBI and the ICRF to study tectonic activity, sea level rise, interactions between Earth's core and mantle, and post-glacial land rebound and subsidence.

The VLBI technique also increased the accuracy of Earth Orientation Parameters (EOP), measurements that precisely characterize irregularities in Earth's rotation, critical for space missions. This includes polar motion, or slight offsets in the axis around which Earth rotates—its wobble. Any significant motion or mass change on Earth's surface can affect its axis or the velocity of its rotation, like earthquakes, large tides or ocean currents, or even melting ice.



Radio telescope stations across the globe that have contributed observations to the determination of the International Celestial Reference Frame (ICRF). The blue triangles indicate International Very Long Baseline Array (VLBI) Service for Geodesy and Astrometry (IVS) stations, while the green dots represent the ten Very Long Baseline Array (VLBA) stations and the three Deep Space Network (DSN) stations. (Courtesy NASA)

Another parameter involves time-keeping standards that measure a day as one rotation of Earth. Because Earth's spin rate varies, the length of each day slightly varies. Of all the space geodetic techniques, only VLBI accurately measures UT1, a form of Universal Time based on the precise rotational position of the Earth. UT1 provides a correction to Coordinated Universal Time (UTC), on which civil time is based. "The UT1 correction changes the most rapidly of the EOP's, so it is necessary to measure it daily," Gordon said.

Accounting for these tiny motions, along with precise time keeping, improve GPS positioning. In fact, without the UT1 measurements provided by VLBI, GPS satellites would not be able to provide accurate locations, Gordon said.

Several NASA Earth Science missions depend on the EOP input from VLBI, in particular UT1. For instance, the Ice, Cloud and land Elevation Satellite 2 (ICESat-2) relies on VLBI-supported data for precise orbit determination.

More radio sources, more accuracy

The first version of this reference frame, the ICRF1, was completed by researchers at a host of international agencies. After being approved by the International Astronomical Union, the ICRF1 was adopted in 1998 and relied on the positions of 608 distant celestial objects. In 1999, the International VLBI Service for Geodesy and Astrometry (IVS) was formed to bring under one roof the operational activities of the geodetic and astrometric VLBI disciplines and to standardize the data flow. The central bureau of the service is hosted at GSFC and Behrend functions as its secretary.

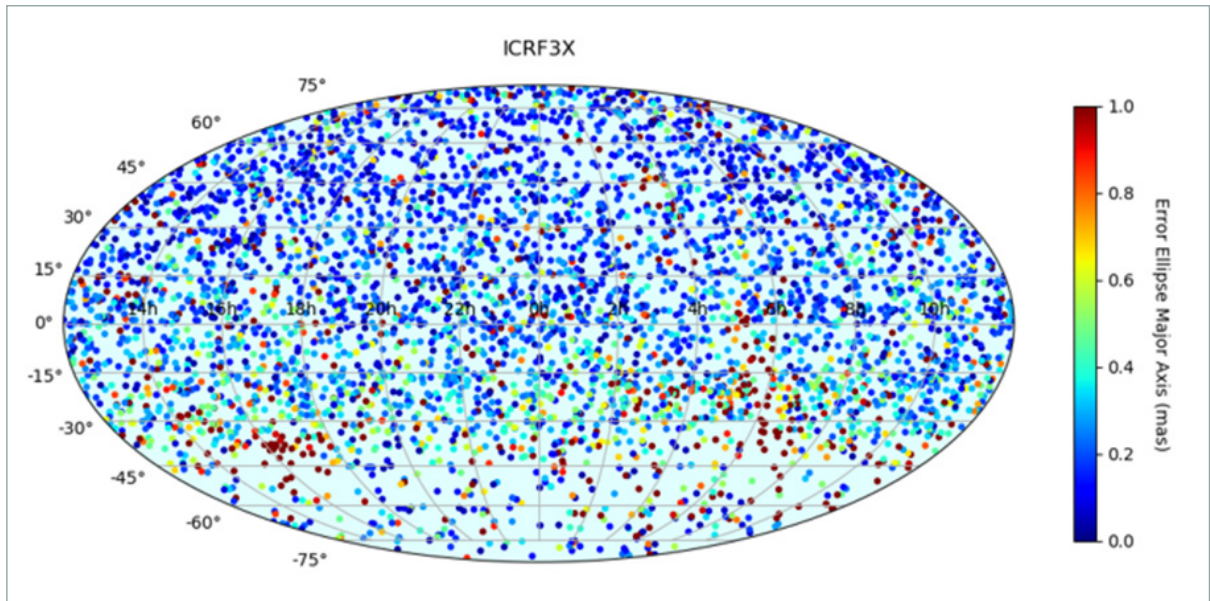


The 26-meter (85-foot) radio telescope at Mt. Pleasant in Hobart, Australia, is part of the globally distributed network of sites that contributed to the third International Celestial Reference Frame (ICRF3). Unlike tubular optical telescopes, radio telescopes are usually composed of an antenna adjacent to or cradled in a large parabolic dish. This structure is designed to channel radio waves from very specific directions—a distant galaxy, for instance. (Courtesy University of Tasmania and Jim Lovell, <https://jimlovellphoto.com>)

In 2009, the ICRF2 was adopted, using 3,414 sources. The ICRF3 becomes official in January 2019, based on 4,536 sources from observations dating to 1979. “The ICRF3 precision is about 30 micro-arc seconds,” Gordon said. “For an analogy, that’s about the size of a billiard ball on the moon as seen from Earth.” Gordon served as a key member of the ICRF3 working group. VLBI data used for the ICRF are archived at CDDIS, and at mirror sites in Europe.

Over the decades, radio telescopes have advanced observations, precisely capturing minute quasar motion. Not only is ICRF3 more accurate, it corrects for aberration: a phenomenon where a stationary object appears to change as you are moving relative to it. This correction accounts for the solar system rotating around the Milky Way, completing a circuit every 225 million years, resulting in a slow drift of distant quasars as seen from Earth. “The motion is only 5.8 micro-arc seconds per year, which is an extremely tiny number, like seeing a penny on the surface of the moon,” Gordon said.

To generate these increasingly accurate terrestrial and celestial references frames, researchers rely on radio waves that have travelled across vast distances of not only space, but time. “The quasars that we are using, they are several billions of light years away. So the signals that we use for the VLBI technique are actually older than the Earth itself,” Behrend said. “I think that’s an amazing thing, that we use something now that was produced so many billions of years ago.”



This plot shows the sky distribution of the 4,536 celestial radio sources used in the International Celestial Reference Frame 3 (ICRF3). Color indicates accuracy of the source positions: blue indicates higher accuracy; red indicates lower accuracy. (Courtesy Sebastien Lambert/Paris Observatory)

For more information

[NASA Crustal Dynamics Data Information System \(CDDIS\)](#)

[NASA Goddard Science and Exploration Directorate](#)

[NASA Space Geodesy Project](#)

[International Celestial Reference Frame \(ICRF\)](#)

[Very Long Baseline Interferometry \(VLBI\)](#)

References

Gordon, D. 2017. Impact of the VLBA on reference frames and Earth orientation studies. *Journal of Geodesy* 91(7): 735-742. doi:10.1007/s00190-016-0955-0

Nothnagel, A., T. Artz, D. Behrend, and Z. Malkin. 2017. International VLBI service for geodesy and astronomy. *Journal of Geodesy* 91: 711-721. doi:10.1007/s00190-016-0950-5

Crustal Dynamics Data Information System (CDDIS). 2018. Very Long Baseline Interferometry (VLBI), International VLBI Service for Geodesy and Astrometry (IVS) products. Available on-line https://cddis.nasa.gov/Data_and_Derived_Products/VLBI/VLBI_data_holdings.html from NASA EOSDIS CDDIS, Greenbelt, MD, U.S.A.

About the remote sensing data	
Sensors	Various radio telescopes
Data sets	Very Long Baseline Interferometry (VLBI), International VLBI Service for Geodesy and Astrometry (IVS) products https://cddis.nasa.gov/Data_and_Derived_Products/VLBI/VLBI_data_holdings.html
Resolution	N/A
Parameter	Very Long Baseline Interferometry (VLBI)
DAAC	NASA Crustal Dynamics Data Information System (CDDIS)

Leaving dry lands behind



Census and climate data uncover internal migration patterns in North Latin America and the Caribbean.

By Natasha Vizcarra

In Central America, maize and bean farmers have mastered an agricultural relay that rides two rainy seasons. Farmers plant maize, or corn, in May, when the first rains arrive. Then a short dry spell called the *canícula* straddles July and August. When the second rainy season arrives in September, farmers plant beans between the rows of maturing maize. The maize is harvested in October, and the beans in November. In sync with land and climate, the method has helped farmers grow these beloved staples for decades.

- [About the data](#)
- [About GES DISC](#)
- [About SEDAC](#)

However, everything hinges on the *canícula*, roughly translated to dog days or high summer. When the *canícula* arrives early, or is drier or lasts longer than usual, it threatens crops in both planting seasons. An unpredictable *canícula* also nixes the possibility of a third planting in humid regions.

In the last decade, recurrent droughts, excessive rains, and flooding have plagued Central America. And in the last four years, a deep drought has settled in, often intensifying the *canícula* and preventing either rainy season from happening at all. In the Dry Corridor, an arid swath of lowlands covering the Pacific Coast from El Salvador to Costa Rica, maize farmers have lost more than 60 percent of their crop, and bean farmers 80 percent. Humanitarian organizations estimate that close to half a million people are vulnerable to moderate to severe food shortage. Reports of people leaving farming areas for jobs in nearby cities and countries have dire implications for the region's food security.

Valerie Mueller, formerly a researcher at the International Food Policy Research Institute in Washington, D.C. and now an assistant professor at Arizona State University, was drawn to the growing crisis in Central America as well as in Mexico and the Caribbean. She had been studying similar drought-related crises in Asia and Africa by probing population and climate data. The drought and migrations in Central America and neighboring countries suggested a strong link between climate and migration. Could the data yield patterns that might help humanitarian organizations find the best way to provide aid?



A maize farmer in El Salvador examines his desiccated soil. (Courtesy Neil Palmer/International Center for Tropical Agriculture)

The power of weighted averages

To start with, Mueller needed a way to estimate the impact of climate events on populations. She worked with colleagues Javier Baez and German Caruso at the World Bank and Chiyu Niu at the University of Illinois, now also with the World Bank, to find the right combination of data sets.

They chose to use a population-weighted average, a common statistical tool to study populations. In this averaging method, instead of each data point contributing equally to a final average, some data points contribute more weight than others. Niu explained, “Let’s say for example, that in the state of North Carolina there are more trees than people and in the state of Virginia there are more people than trees. Then a storm hits both areas with heavy rainfall. Because we’re studying the impact of the storm on human beings, rather than trees we want, Virginia to weigh more because there are more people there than in North Carolina.”

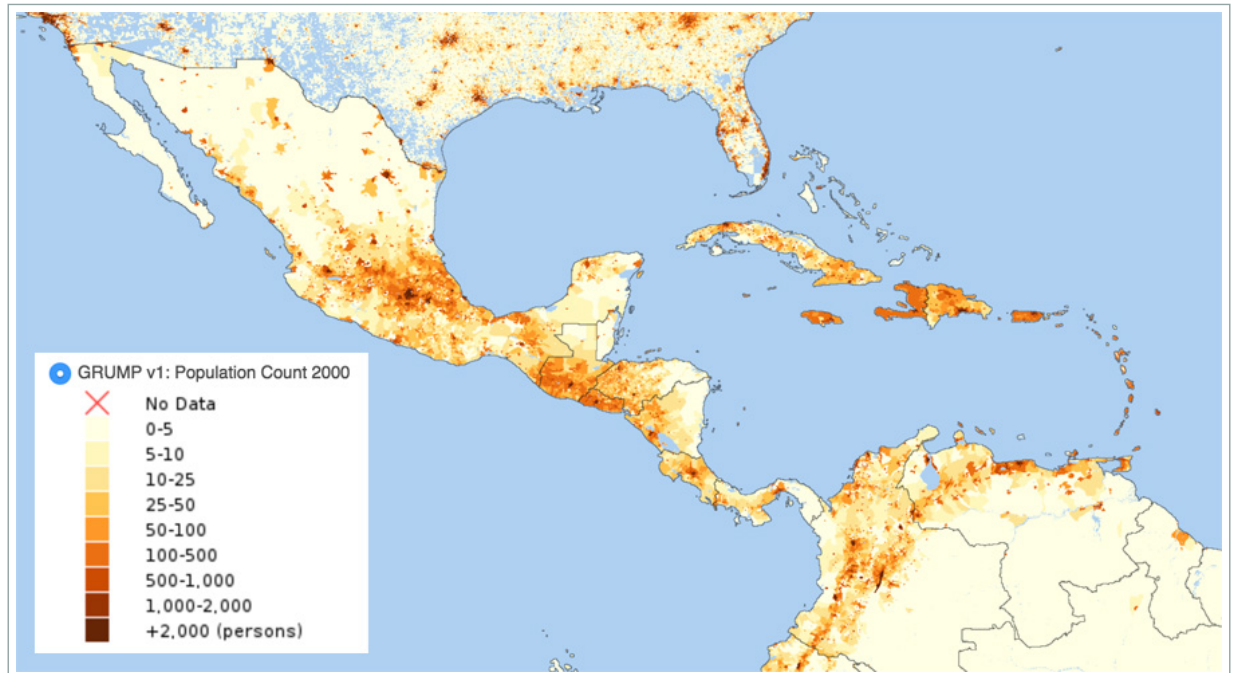
Mueller added, “Population-weighted averages allow us to place more weight and attention on shock that happened in grids that are highly populated. That’s where we expect the climate exposure to happen.” To calculate population-weighted averages for all provinces in their study area, they downloaded population data from NASA’s Socioeconomic Data and Applications Center (SEDAC). The data are organized using a geographical grid, which makes them easier to link with satellite and other climatic data. This way, researchers can study how certain environmental factors affect different locations.

Mueller and her colleagues combined the averages with temperature and rainfall records to generate historical rainfall and temperature data for all provinces in their study area. They also combined the averages with daily rainfall data from NASA’s Tropical Rainfall Measuring Mission (TRMM) to identify hurricanes that affected the populations, and with data from the International Disaster Database (EM-DAT) to identify droughts. The researchers also tapped numbers on gross domestic product per capita and aid culled from the World Bank.

Finally, the researchers needed census records that included migration status, or whether the person migrated from somewhere within the last five years prior to the census; the age of the person at the time of the survey; and details about the person’s sex and education. They could only find useable census records for Costa Rica,

Dominican Republic, El Salvador, Haiti, Jamaica, Mexico, Nicaragua, and Panama, so they limited the study to those countries. The census years ranged from as early as 1982 to as recent as 2011.

When they analyzed the census records alone, they found that over a five-year period, 5 percent of the population within each of the countries had moved across provinces. When they combined the census data with the population-weighted climatic data, more details emerged about which part of the population was moving and why.



This map shows population count grid data for North Latin America and the Caribbean for 2000 from the NASA Socioeconomic Data and Applications Center (SEDAC). SEDAC population data are organized using a geographical grid, which makes them easier to link with satellite and other data. (Courtesy SEDAC)

Departures in the data

Mueller and her colleagues found that younger people, ranging from 15 to 35 years old, are more likely to migrate to other provinces in response to disasters, especially droughts. “One reason is that if the household’s head leaves, it’s probably more devastating to local production than if an adolescent left,” Mueller said. “They don’t have strong property rights in a lot of these places. If someone as significant to the household as the head leaves, there’s a fear that the land will be expropriated, or taken by the government—ostensibly to be used for the public good.”

The findings suggested that young migrants were likely to relocate to rural and small-town settings, possibly for off-farm jobs. “This may be because the young migrants may not have enough money to move to farther urban areas,” Mueller said.

Their analysis also showed that youth from wealthier countries are more likely to migrate to other provinces in the wake of a drought than a hurricane. Although the analysis could not explain why, Mueller and her colleagues have theories. People lose jobs because there are no seedlings to plant, no growing crops to fertilize or care for, or nothing to harvest at season’s end. So a drought increases the number of people who need jobs.

“Wealthier countries can accommodate this increase in the supply of workers caused by a drought,” Mueller said. It seems counterintuitive then that these young people in wealthier countries would still choose to leave during a drought, but when they can no longer find jobs in their local communities, they can still find jobs outside of agriculture elsewhere in the country. Young people in poorer countries do not have that choice.



A maize farmer in Nicaragua takes a break from preparing his field for the planting season. (Courtesy Neil Palmer/International Center for Tropical Agriculture)

Trapped populations

"In poor countries, you might see that migration goes down because the demand for seasonal or other forms of employment declines with exposure to a climatic shock," Mueller said. "This has been referred to as the 'trapped population dynamic.'" Researchers describe the dynamic as the double set of risks that poor populations face when dealing with an environmental threat: they are unable to move away from these threats, and poverty makes them especially vulnerable to environmental changes.

Finally, Mueller and her colleagues found that targeted aid appears to mediate the exodus of young people from drought-stricken areas. "We've seen that people are not necessarily more likely to migrate in response to a natural disaster because a country's social protections target households in areas that are vulnerable to that specific disaster," Mueller said.

Mueller cited her previous study on Pakistan where social protection programs target areas prone to flooding. In that study, she saw that people were also likely to migrate because of a drought rather than flooding. "We posit that one of the reasons why they might not be migrating because of the floods was because they lived in areas that are prone to flooding and that they were receiving stipends during that event," she said.

"Our findings highlight the importance of social protection and regional planning policies to reduce the vulnerability of youth to droughts in the future," Mueller said. "Social protections may play a strong role in reducing environmental displacement for these young people."



After ten months without proper rains in 2015, Haiti's countryside markets are abandoned. As crops failed, villagers had few products left to trade, eat, or drink. (Courtesy European Civil Protection and Humanitarian Aid Operations)

For more information

[NASA Goddard Earth Sciences Data and Information Services Center \(GES DISC\)](#)

[NASA Socioeconomic Data and Applications Center \(SEDAC\)](#)

[Global Rural-Urban Mapping Project \(GRUMP\), v1](#)

[Tropical Rainfall Measuring Mission \(TRMM\)](#)

References

Baez, J., G. Caruso, V. Mueller, and C. Niu. 2017. Droughts augment youth migration in Northern Latin America and the Caribbean. *Climatic Change* 140(3): 423-435. [doi:10.1007/s10584-016-1863-2](#)

Black, R., S. R. G. Bennett, S. M. Thomas, and J. R. Beddington. 2011. Climate change: Migration as adaptation. *Nature* 478: 447-449, [doi:10.1038/478477a](#)


Center for International Earth Science Information Network (CIESIN) Columbia University, International Food Policy Research Institute—IFPRI, The World Bank, and Centro Internacional de Agricultura Tropical—CIAT (2011) Global Rural-Urban Mapping Project, Version 1 (GRUMPv1): population count grid. Palisades, NY: NASA Socioeconomic Data and Applications Center (SEDAC). [doi:10.7927/H4VT1Q1H](#)


Minnesota Population Center. 2015. Integrated Public Use Microdata Series, International: Version 6.4. Minneapolis: University of Minnesota. [doi:10.18128/D020.V6.4](#)






Mueller, V., C. Gray, and K. Kosec. 2014. Heat stress increases long-term human migration in rural Pakistan. *Nature Climate Change* 4: 182-185. [doi:10.1038/nclimate2103](#)

Tropical Rainfall Measuring Mission (TRMM). 2011. TRMM Combined Precipitation Radar and Microwave Imager Rainfall Profile L2 1.5 hours V7, Greenbelt, MD, Goddard Space Flight Center Earth Sciences Data and Information Services Center (GES DISC). https://disc.gsfc.nasa.gov/datacollection/TRMM_2B31_7.html

Tropical Rainfall Measuring Mission (TRMM). 2010. TRMM .25 deg x .25 deg Gridded Precipitation Text Product, Greenbelt, MD, Goddard Space Flight Center Earth Sciences Data and Information Services Center (GES DISC). <ftp://trmmopen.gsfc.nasa.gov/pub>.

Tropical Rainfall Measuring Mission (TRMM). 2011. TRMM Microwave Imager Hydrometeor Profile L2 1.5 hours V7, Greenbelt, MD, Goddard Space Flight Center Earth Sciences Data and Information Services Center (GES DISC). https://disc.gsfc.nasa.gov/datacollection/TRMM_2A12_7.html .

Tropical Rainfall Measuring Mission (TRMM). 2011. TRMM Precipitation Radar Rainfall Rate and Profile L2 1.5 hours V7, Greenbelt, MD, Goddard Space Flight Center Earth Sciences Data and Information Services Center (GES DISC). https://disc.gsfc.nasa.gov/datacollection/TRMM_2A25_7.html .

About the data			
Data set	Population Count Grid, v1 (1990, 1995, 2000)  , from the Global Rural-Urban Mapping Project (GRUMP), v1 		
Resolution	30 arc-seconds, latitude/longitude		
Parameter	Population count		
DAAC	NASA Socioeconomic Data and Applications Center (SEDAC)		
About the remote sensing data			
Satellite	Tropical Rainfall Monitoring Mission (TRMM)	TRMM	TRMM
Sensors	TRMM Microwave Imager (TMI)	Precipitation Radar	Precipitation Radar, Microwave Imager
Data sets	TRMM Microwave Imager Hydrometeor Profile L2 1.5 hours V7 (TRMM_2A12) 	TRMM Precipitation Radar Rainfall Rate and Profile L2 1.5 hours V7 (TRMM_2A25) 	TRMM Combined Precipitation Radar and Microwave Imager Rainfall Profile L2 1.5 hours V7 (TRMM_2B31) 
Resolution	5.1 x 5.1 kilometer	4 x 4 kilometer	5 x 5 kilometer
Parameters	Atmospheric water vapor, clouds, precipitation	Precipitation	Clouds, precipitation
DAAC	NASA Goddard Earth Sciences Data and Information Services Center (GES DISC)	NASA GES DISC	NASA GES DISC
<p>The study uses the TRMM data set 3G68, which is an hourly gridded product containing TRMM_2A12, TRMM_2A25, and TRMM_2B31. This non-standard data set is available from GES DISC via ftp://trmmopen.gsfc.nasa.gov/pub.</p>			

Researchers revise the story behind Puerto Rico's 2015 drought.

By Agnieszka Gautier

When Puerto Rico initiated water rations in May 2015, its residents got creative. Children bathed in buckets. Families captured the initial cold water in their showers to fill toilet tanks, where they would then wash their hands on the days the water utility turned off the tap. Depending on where you lived, water was turned off for 24 or 48 hours and then back on for 24 hours. Pitchers, cisterns, and other plastic containers cluttered homes, yards, even rooftops to compensate for those dry tap days.

- [About the data](#)
- [About GES DISC](#)
- [About ORNL DAAC](#)

Most major national and international media outlets blamed the 2015 drought on El Niño, the warm phase of a weather oscillation often associated with drought. The Puerto Rican National Weather Service, however, kept discussing the role of the Saharan Air Layer (SAL) in their daily forecasts. This piqued Thomas Mote, a climate scientist from the University of Georgia, because El Niño did not seem like a reasonable explanation.

The drought really hit eastern Puerto Rico and the early rain season, affecting April, May, and June. If El Niño interferes with weather, which it rarely does in the eastern Caribbean, it would do so during the hurricane season in late summer and into fall. To weed out the culprit behind the 2015 drought, Mote needed to model the weather patterns around Puerto Rico. The challenge, however, was that most precipitation models are geared for the mid latitudes, where the mechanisms driving weather are fundamentally different from the tropics. So Mote and his team needed to find a tool that could measure thunderstorm potential specifically for the tropics. Then they could consider if the SAL played a significant part in the drought.



A National Guard member opens a portable military water tank, which is used to distribute potable water to communities affected by the 2015 drought. (Courtesy thenationalguard/Flickr)

Current disasters

It had been 20 years since a drought hit Puerto Rico, but 2015 was extreme - a category the US Drought Monitor defines as having major crop and pasture losses and widespread water shortages. At its peak in August, 74 of its 77 municipalities rationed water. Losing paying customers cost the Puerto Rico Aqueduct and Sewer Authority \$15 million a month.

For an island already hardened by economic struggles, and \$73 billion in debt, Puerto Rico faced record-low rainfall and crumbling water infrastructure: dams in disrepair, silt-blocked reservoirs, and leaky pipelines that lost more than half of the water they transported. Many of these US citizens not only blamed nature, but also politics for the despairing situation. In terms of low rainfall, however, local meteorologists got it right.

When summarizing daily climate drivers for their forecast, Puerto Rican meteorologists often mentioned the SAL. Mote noted their use of the Gálvez-Davison Index (GDI), an experimental tool designed by the Weather Prediction Center, part of the National Oceanic and Atmospheric Administration (NOAA), to better forecast precipitation in the tropics and Caribbean. This index estimates convection, or the likelihood of a thunderstorm brewing in the tropics. Craig Ramseyer, a professor at Salisbury University in Maryland, calculated the prospect for rain using the GDI for April, May, and June of 2015, when the atmosphere should be volatile enough for rain to form. Instead, it was quite stable. "What was interesting about it was when we visualized the convective signal, it had a very coherent pathway back to Africa," Ramseyer said. "And we were like, 'Wow, that should be associated with the Saharan Air Layer.'"

The SAL is an extremely hot, dry swath of dust streaming along in the upper atmosphere. "It's kind of like a fire hose that's getting sprayed out of Saharan Africa and into the eastern Caribbean," Ramseyer said. It often glides a few kilometers above the Atlantic Ocean on top of more humid air. The atmosphere, like the ocean, is composed of currents. Moist currents must rise easily and rapidly for thunderstorm formation. But in the Caribbean and tropics at large, another key component for rain is a temperature phenomenon called the trade wind inversion, basically a lid of warm air. "I like to visualize the inversion as depth," Ramseyer said. A strong, deep lid prevents

upward mobility and no thunderstorms will form. Mote said, “Normally, the inversion layer is weak enough that thunderstorms can build through the warmth and continue to develop through it.”



La Perla, the poorest neighborhood in San Juan, Puerto Rico, pops with color. The drought mainly affected the eastern, more populated portion, including San Juan, burdening the lives of 2.5 million of Puerto Rico's 3.5 million population. (Courtesy khowaga/Flickr)

Root origins

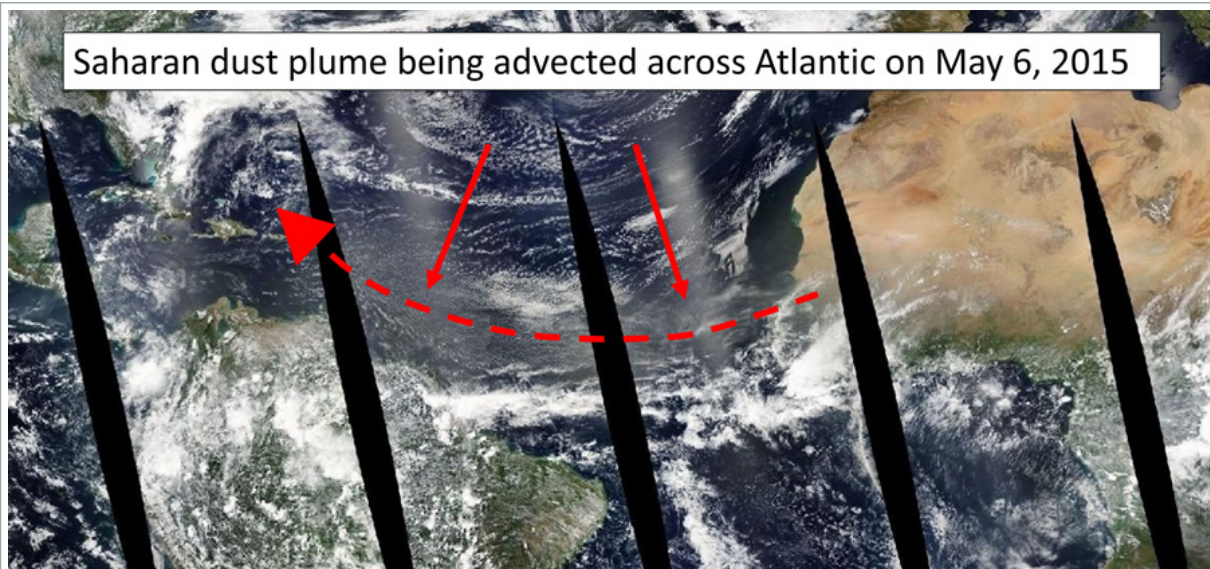
In the spring of 2015, the sky over San Juan - Puerto Rico's capital - turned hazy. It looked like smog, but residents were familiar with the dust coming out of Africa. The Sahara Desert is Earth's largest desert, almost the size of the continental United States. Each year rising dust forms massive plumes visible from space, though dust particles themselves are tiny - no more than a tenth of the width of a human hair.

The SAL rides right along the trade wind inversion. The GDI measures the magnitude of the trade wind inversion - deeper inversions hint that the SAL is more active. “It is not a definitive causality but it certainly suggests the SAL is at play,” Ramseyer said. Prior to the development of the GDI, climate indexes signaled rain, but no actual thunderstorms would form. “The environment and the atmosphere have sort of different ingredients needed in the tropics versus the mid latitudes,” Ramseyer said. “In the middle latitudes, for example, what's happening up at about 30,000 to 40,000 feet is very important in thunderstorm formation; in the tropics, we don't need that.” So models of the tropics could not properly incorporate the SAL.

To get to the root of the 2015 drought, Mote's team first detected if and when the inversion was getting stronger. If it was, then they needed observations from the Ozone Monitoring Instrument (OMI) on the NASA Aura satellite, and specifically its Aerosol Index (AI) data, to find dust was present in the atmosphere. NASA's Goddard Earth Sciences Data and Information Services Center (GES DISC) stores AI data, which measures minuscule atmospheric particles by calculating the difference between the amount of ultraviolet light scattering in a dust-filled and non-dust-filled atmosphere. But what degree of dust was out of the ordinary?

“April, May, and June typically have lots of dust in the atmosphere, so we needed to see if the Saharan Air Layer made any difference,” Ramseyer said. To compare, he first needed to know what was normal for early spring in Puerto Rico. The team went back as far as the satellite data could take them—to the early 2000s—determining average dust levels for aerosols in the sky for every day in spring.

Saharan dust plume being advected across Atlantic on May 6, 2015



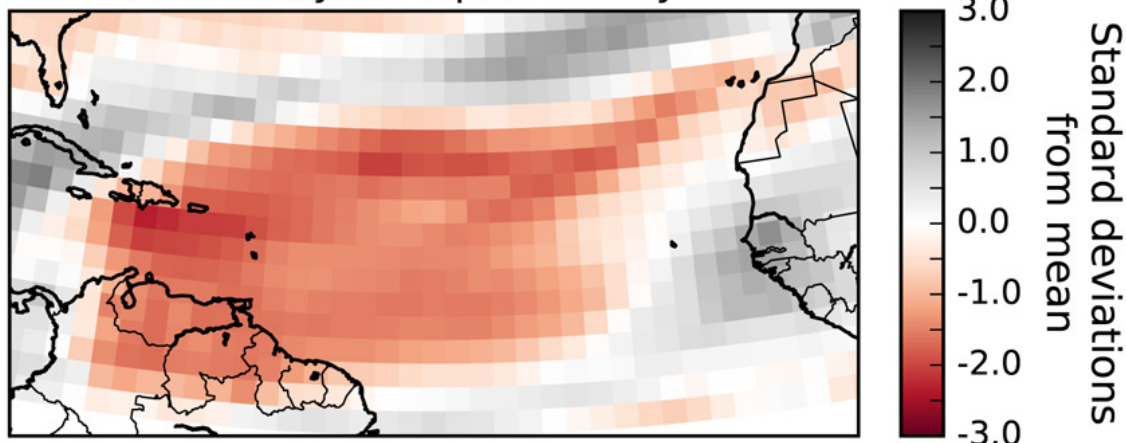
This image shows a true color composite of a Saharan dust plume crossing the Atlantic Ocean on May 6, 2015. Data are from the Moderate Resolution Imaging Spectroradiometer (MODIS) sensor on the NASA Terra satellite. (Courtesy NASA)

The a-ha moment

After establishing a baseline for spring conditions, the team found that dust levels in 2015 were 50 percent higher than normal for April, May, and June. "I was surprised to see such a robust signal," Mote said. That extra dust absorbs solar radiation in the atmosphere, warming the trade wind inversion further, and capping the rise of moisture needed for thunderstorm formation. The tropics have a dry season, typically winter in the Northern Hemisphere, and a wet season in early spring and late summer or early fall, corresponding with the hurricane season. "What was unique about 2015, and we think other years where we see a drop in the early rainfall season, is that the SAL comes across the Atlantic sooner than normal," Mote said.

The researchers cannot yet say why the SAL arrived earlier than usual in 2015 or other early season drought years, but think this would be a fruitful area of scholarship. "Good aerosol data are still fairly limited," Mote said. "We can't go back and recreate what we didn't have, so we look forward to the time when we'll have even longer records of ground- and satellite-based products of aerosols." As for Ramseyer, he was surprised by how little awareness exists among a lot of research bodies about the importance of the SAL in the eastern Caribbean. "Sometimes climatologists, in particular, fall back on the El Niño stuff. And for us to be able to tell them about the SAL being a key piece was kind of an a-ha moment."

GDI Anomaly: 30 April - 5 May 2015



This map shows departure from average Gálvez-Davison Index (GDI) values, or the magnitude of trade wind inversion, for the week of April 30 to May 5, 2015, as expressed in standard deviations to illustrate the significance of these differences. Trade wind inversion is a temperature phenomenon specific to the tropics responsible for potential thunderstorm formation. Red contours represent a stronger inversion compared to the monthly average; Grey contours represent a weaker inversion compared to the monthly average. At the end of April, the trade wind inversion intensified over the eastern Caribbean and South America, deviating far its average magnitude. (Courtesy T. Mote, et al., 2017, *Journal of Geophysical Research*)

For more information

[NASA Goddard Earth Sciences Data and Information Services Center \(GES DISC\)](#)

[NASA Oak Ridge National Laboratory Distributed Active Archive Center \(ORNL DAAC\)](#)

[Daymet](#)

[NASA Ozone Monitoring Instrument \(OMI\)](#)

References

Hovila, J., A. Arola, and J. Tamminen. 2007. OMI/Aura Surface UV Irradiance 1-orbit L2 Swath 13x24 km V003, Greenbelt, MD, USA, Goddard Earth Sciences Data and Information Services Center (GES DISC). [doi:10.5067/Aura/OMI/DATA2027](https://doi.org/10.5067/Aura/OMI/DATA2027)

Mote, T. L., C. A. Ramseyer, and P. W. Miller. 2017. The Saharan Air Layer as an early rainfall season suppressant in the eastern Caribbean: The 2015 Puerto Rico drought. *Journal of Geophysical Research: Atmospheres*, 122: 10,966-10,982. [doi:10.1002/2017JD026911](https://doi.org/10.1002/2017JD026911)

NOAA Weather Prediction Center. 2016. Experimental Gálvez-Davison Index (GDI), accessed 2 April 2017. <http://www.wpc.ncep.noaa.gov/international/gdi>

Ramseyer, C. A. and T. L. Mote. 2016: Atmospheric controls on Puerto Rico precipitation using artificial neural networks. *Climate Dynamics* 47: 2,515-2,526. [doi:10.1007/s00382-016-2980-3](https://doi.org/10.1007/s00382-016-2980-3)

Thornton, P.E., M. M. Thornton, B. W. Mayer, Y. Wei, R. Devarakonda, R. S. Vose, and R. B. Cook. 2018. Daymet: Daily Surface Weather Data on a 1-km Grid for North America, Version 3. ORNL DAAC, Oak Ridge, TN, USA. [doi:10.3334/ORNLDAAC/1328](https://doi.org/10.3334/ORNLDAAC/1328)

About the remote sensing data		
Satellite	Aura	
Sensors	Ozone Monitoring Index	Various meteorological sensors
Data sets	OMUVB: OMI/Aura Surface UV Irradiance 1-orbit L2 Swath 13 x 24 km V003	Daymet v3
Resolution	13 x 24 kilometer	1 x 1 kilometer
Parameters	Irradiance	Temperature, precipitation occurrence and amount, humidity, shortwave radiation, snow water equivalent, and day length
DAACs	NASA Goddard Earth Sciences Data and Information Services Center (GES DISC)	NASA Oak Ridge National Laboratory (ORNL) Distributed Active Archive Center (DAAC)

Paving a new lifestyle



As rapid urbanization transforms India's landscape, doctors face a new set of challenges in protecting public health.

By Michon Scott

Throughout the 20th century, familiar illnesses in India included communicable diseases such as malaria or typhoid, diseases affecting expectant mothers and newborns, and diseases stemming from inadequate nutrition. Shortly after the turn of the 21st century, the nation's disease burden shifted. Although communicable illnesses remain a daunting problem, the diseases most likely to cause disability and death now are noncommunicable, such as heart disease and diabetes.

- [About the data](#)
- [About LAADS DAAC](#)
- [About LP DAAC](#)

In short, India has made what health experts call the epidemiological transition - from a state of high mortality among infants and children, and epidemics affecting all age groups, to a state of diseases affecting primarily older individuals, such as hypertension. One part of the country where this transition happened early is in the southern state of Tamil Nadu, and particularly in the state's capital city of Chennai (formerly Madras), along India's southeastern coast.

Mohan Thanikachalam, now based at Tufts University, was born in Chennai. He left home for medical training in the United States and returned a cardiac surgeon. Thanikachalam came home to a changed hometown facing a different set of health risks, similar to what doctors see in developed nations. He soon realized that, though surgical intervention can save a life, Chennai needed a public-health intervention to save many lives. Such an intervention would need data. "With cardiovascular disease, most of the data come from the United States or Europe," Thanikachalam said. "India has a completely different population." Heart disease and diabetes are often related to obesity. "But the population in India, at least the people I saw, they were not necessarily obese, so I was really surprised to see the extent of diabetes," he said.

No one has all the answers as to why India's population has seen such a rapid increase in lifestyle disease, but something else has happened over roughly the same time period: urbanization. According to the World Bank, in 1960, India's urbanites comprised just under 18 percent of the country's population; in 2016, that number had climbed to over 33 percent. With a total population of over 1.3 billion, India now has an urban population of over 400 million. That is more than the entire population of the United States. Thanikachalam's hometown of Chennai currently has more than 7 million residents, and it is projected to top 10 million by 2030.



Chennai residents cross a well-lit crosswalk at night. (Courtesy K.G. Suriya Prakash/Wikimedia)

Urbanization does not just change the landscape, it changes people's lives, starting with the air they breathe. "Pollution is one of the top risk factors for mortality in India," Thanikachalam said. He described other ways that urbanization affects residents. "We know that urban populations have higher body mass indexes, and they take in more calories. We also know they have lower physical activity. And we know they have higher stress levels. When we measure the level of anxiety, the levels are higher in the urban population." At present, researchers can only speculate about the causes of higher stress among city dwellers, but Thanikachalam suspects that social changes brought about by urbanization play a part.

To get a better handle on risk factors for heart disease, Thanikachalam and some of his colleagues designed a study to assess the population's health. The Population Study of Urban, Rural and Semiurban Regions for the Detection of Endovascular Disease and Prevalence of Risk Factors and Holistic Intervention Study (PURSE-HIS) examined more than 8,000 people between 2009 and 2011. Researchers randomly selected study participants from Chennai and nearby semiurban and rural communities. Through a combination of home visits and clinic appointments, the study team assessed risk factors for future cardiologic and metabolic disease, as well as demographic and lifestyle factors. Participants underwent a battery of tests, including blood samples, urine samples, electrocardiograms (EKG), even treadmill tests. They also answered questions about physical activity and stress.

The PURSE-HIS study provided a detailed snapshot of the population's risk factors. But to see how the landscape was changing, Thanikachalam embarked on a new study involving remote sensing. One of his collaborators was Kevin Lane at Boston University. With a background in biology, urban planning, and political science, Lane specializes in the study of how environment affects public health. "I've always been interested in the intersection between science and policy," Lane said. "In these places that rapidly undergo urbanization, you can actually see the changes occurring, and how that could potentially be associated with health outcomes."



Part of the PURSE-HIS protocol included an assessment of each participant's diet. A researcher and participant discuss nutrition. (Courtesy Mohan Thanikachalam)

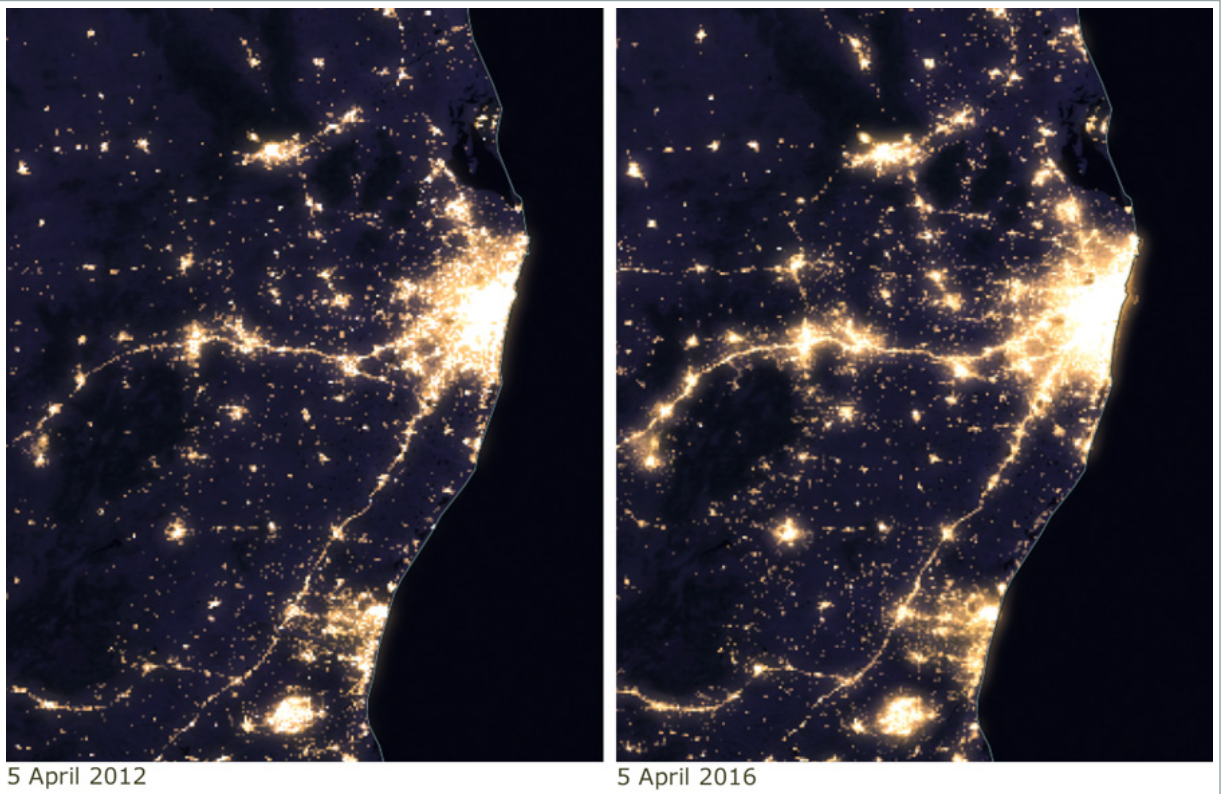
Seeing risk through satellites

In addition to the results of the PURSE-HIS study, Lane, Thanikachalam, and their coauthors examined multiple facets of the physical environment in and around Chennai. They incorporated paved surfaces derived from Landsat 5 Thematic Mapper images acquired in February and May 2009. They estimated nighttime lights from a cloud-free composite acquired in January 2013 by the Visible Infrared Imaging Radiometer Suite (VIIRS) on the joint NASA/NOAA Suomi National Polar-Orbiting Partnership (Suomi-NPP) satellite, available from NASA's Level-1 and Atmosphere Archive and Distribution System (LAADS) Distributed Active Archive Center (DAAC) at NASA's Goddard Space Flight Center. And they examined greenness by incorporating two 16-day composites, acquired in February and June 2009, by NASA's Moderate Resolution Imaging Spectroradiometer (MODIS). This Normalized Difference Vegetation Index (NDVI) product is available from NASA's Land Processes DAAC (LP DAAC).

Combining all the data sources, Thanikachalam, Lane, and their coauthors found that people living in more urbanized environments—with less vegetation, more paved surfaces, and more nighttime light pollution—had higher blood pressure.

We all have a chronological age measured in the years, months, and days since birth. We also all have a biological age driven by the wear and tear experienced throughout life. Factors such as diet, exercise, air quality, smoking, and local environment affect biological age, which can outpace chronological age in unhealthy environments. An unhealthy environment can drive early vascular aging, which can lead to an early onset of cardiovascular disease. Lane and Thanikachalam's research supports a growing body of evidence that a reduction in vegetation around one's home can accelerate vascular aging. Such environmental changes can lead to other changes, such as less healthy eating habits, loss of social cohesion, and more noise and air pollution.

Peter James, assistant professor at the Harvard Medical School Department of Population Medicine, who was not involved in this research, said, "Few prior studies have been able to examine so many objectively measured environmental factors in concert, and to link these data to objective measures of vascular function is unique. I know of no prior studies examining nighttime lights or impervious surfaces and cardiovascular markers."



This NASA Black Marble comparison shows nighttime lights of Chennai and the surrounding region from 2012 (left) and 2016 (right). Although the same pattern of lights predominates in both images, the lights intensify over just four years, indicating increased urbanization. Data are from the Visible Infrared Imaging Radiometer Suite (VIIRS) instrument aboard the NASA Suomi National Polar Orbiting Partnership (NPP) satellite. Explore these images using Worldview (left image: <https://go.nasa.gov/2Ei6XKg> ; right image: <https://go.nasa.gov/2RMAUEN>). (Courtesy NASA Worldview)

Looking toward the future

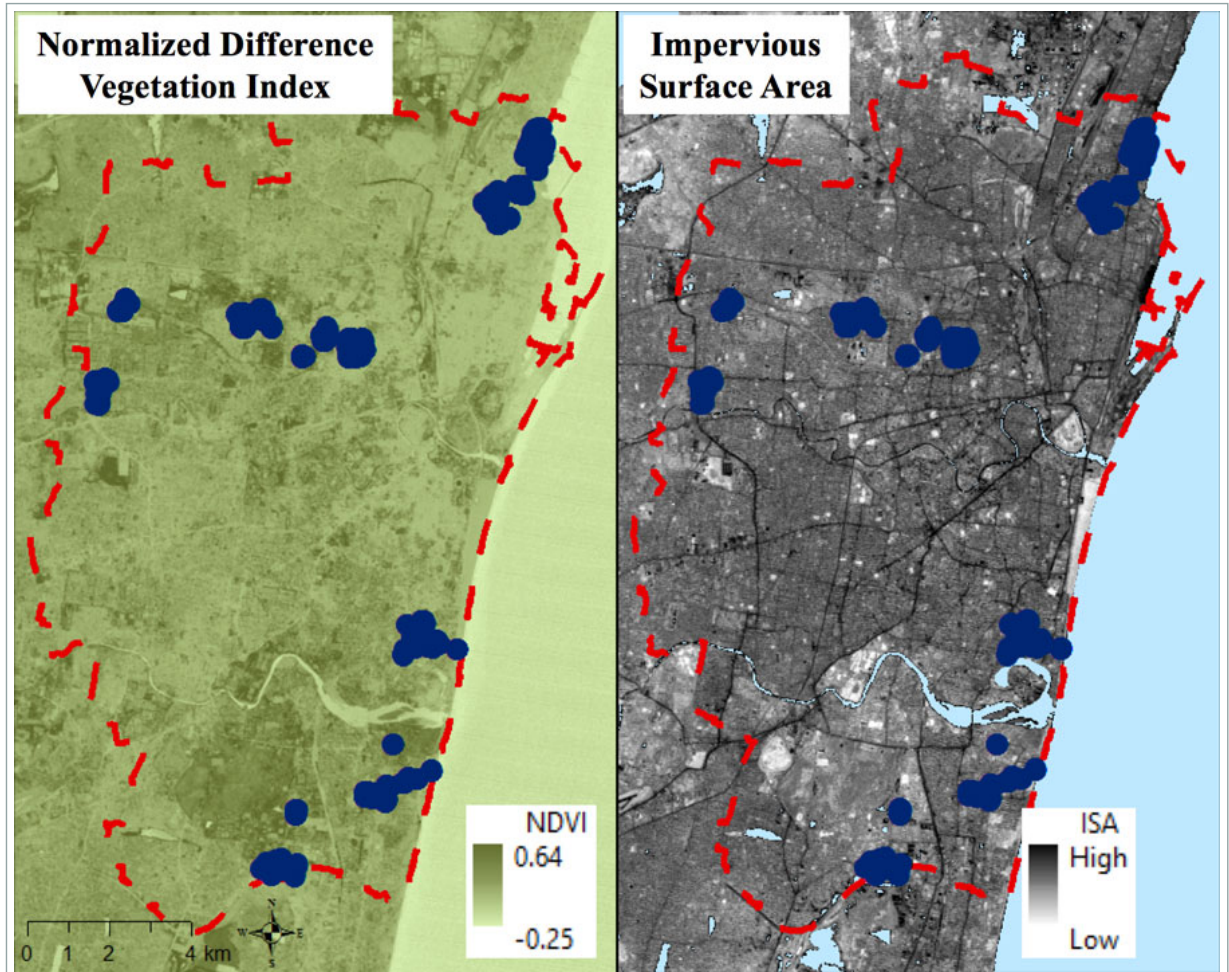
Lane and Thanikachalam consider this study one more step up a tall staircase, and they acknowledge the study's limitations. Lane explained that the NDVI data simply indicates photosynthetic activity. "But we're not able to easily distinguish the type of vegetation that people would have in these areas. It indicates amount of greenness around a person's home but it could be trees or bushes or grass," he said. "Another limitation of our study is that it's one snapshot, one point in time." Studies that follow human subjects and environmental changes over time will yield more insights. Further research might shed more light on the relationship between urbanization and physical activity, as the results from this study were surprisingly mixed.

Perhaps the greatest drawback of the study was that the study unit was the household rather than the individual. Some household members, young males of working age in particular, are exposed to a microenvironment somewhere else. "If you don't take into account where somebody is spending significant amounts of time away from home, that's what's known as exposure misclassification," Lane said.

Even partial insights can point to meaningful changes. In his original PURSE-HIS study, Thanikachalam examined the potential of two systems of medicine to intervene. One is modern Western medicine, and the other is Siddha medicine. Among the oldest systems of medicine in the country, Siddha is popular in southern India. As it can drive healthier lifestyle choices, it may provide an effective solution. "It's related to the culture," Thanikachalam said. "For an average 60-year-old Indian woman with diabetes hypertension, you'll probably get more buy-in by looking at yoga and a more traditional diet versus asking her to go to a gym and run on a treadmill. I think the way we are trying to approach it as the best of both worlds."

Whichever treatment avenue prevails, early identification of risk factors and early intervention offer the most promise. Thanikachalam noted that 50 to 60 percent of the PURSE-HIS study population had high blood pressure and did not know it. As in the developed world, they showed no symptoms. "Once you get diagnosed with high

blood pressure or diabetes, that's almost end-stage disease. It's very difficult to cure it," he said. "There should be more focus on earlier changes so that intervention can make a difference.



Researchers combined measurements to assess the landscape and its effect on human health. In the left map, which measures greenness, greener areas indicate more vegetation. In the map on the right, darker areas indicate higher amounts of impervious surface area. Note the inverse relationship between greenness and impervious surface area. The blue circles show residential locations where researchers conducted the Population Study of Urban, Rural and Semiurban Regions for the Detection of Endovascular Disease and Prevalence of Risk Factors and Holistic Intervention Study (PURSE-HIS). (Courtesy Kevin Lane)

For more information

[NASA Land Processes Distributed Active Archive Center \(LP DAAC\)](#)

[NASA Level-1 and Atmosphere Archive and Distribution System \(LAADS\) DAAC](#)

[Landsat 5 Thematic Mapper \(TM\)](#)

[NASA Moderate Resolution Imaging Spectroradiometer \(MODIS\)](#)

[Visible Infrared Imaging Radiometer Suite \(VIIRS\)](#)

References

Didan, K. 2015. MOD13Q1 MODIS/Terra Vegetation Indices 16-Day L3 Global 250m SIN Grid V006. NASA Land Processes Distributed Active Archive Center (LP DAAC). doi:[10.5067/MODIS/MOD13Q1.006](https://doi.org/10.5067/MODIS/MOD13Q1.006).

India State-Level Disease Burden Initiative Collaborators. 2017. Nations within a Nation: Variations in Epidemiological Transition across the States of India, 1990–2016 in the Global Burden of Disease Study. *The Lancet* 390(10111): 2437-2460. doi:[10.1016/S0140-6736\(17\)32804-0](https://doi.org/10.1016/S0140-6736(17)32804-0).

Lane, K.J., E.C. Stokes, K.C. Seto, S. Thanikachalam, M. Thanikachalam, and M.L. Bell. 2017. Associations between Greenness, Impervious Surface Area, and Nighttime Lights on Biomarkers of Vascular Aging in Chennai, India. *Environmental Health Perspectives*. doi:10.1289/EHP541 [↗](#).

Prabhakaran, D., P. Jeemon, and A. Roy. 2016. Cardiovascular diseases in India: Current epidemiology and future directions. *Circulation* 133: 1605-1620. doi:10.1161/CIRCULATIONAHA.114.008729 [↗](#).

Thanikachalam, S., V. Harivanzan, M.V. Mahadevan, J.S.N. Murthy, C. Anbarasi, C.S. Saravanababu, A. Must, R.R. Baliga, W.T. Abraham, and M. Thanikachalam. 2015. Population Study of Urban, Rural, and Semiurban Regions for the Detection of Endovascular Disease and Prevalence of Risk Factors and Holistic Intervention Study: Rationale, Study Design, and Baseline Characteristics of PURSE-HIS. *Global Heart* 10(4): 281-289. doi:10.1016/j.gheart.2014.11.002 [↗](#).

VCST Team. 2016. VIIRS/NPP Day/Night Band 6-Min L1B Swath 750m. NASA Level-1 and Atmosphere Archive and Distribution System (LAADS) Distributed Active Archive (DAAC). doi:10.5067/VIIRS/VNP02DNB.001 [↗](#).

World Bank. Urban population percent of total. <https://data.worldbank.org/indicator/SP.URB.TOTL.IN.ZS?end=2016&locations=IN&start=1960> [↗](#).

About the remote sensing data		
Satellites	Terra	Suomi National Polar-orbiting Partnership
Sensors	Moderate Resolution Imaging Spectroradiometer (MODIS)	Visible Infrared Imaging Radiometer Suite (VIIRS)
Data sets	MODIS/Terra Vegetation Indices 16-Day L3 Global 250m SIN Grid (MOD13Q1) ↗	VIIRS/NPP Day/Night Band 6-Min L1B Swath 750m (VNP02DNB) ↗
Resolution	250 meter	750 meter
Parameters	Normalized Difference Vegetation Index (NDVI)	Infrared radiance, reflected radiance, visible radiance
DAACs	NASA Land Processes Distributed Active Archive Center (LP DAAC)	NASA Level-1 and Atmosphere Archive and Distribution System (LAADS) Distributed Active Archive (DAAC)

Striking new ground



Lightning is much more complex - and extreme - than you think.

By Laura Naranjo

As legend goes, inventor, author, and diplomat Benjamin Franklin discovered electricity in 1752 when he tied a key to a kite string and flew the kite in a thunderstorm to attract lightning. Some historians debate whether Franklin actually conducted the experiment, which he described in a letter to the *Pennsylvania Gazette*. Had Franklin's kite been struck, he would have been electrocuted. Instead, the metal key channeled ambient electricity in the stormy air. Neither did Franklin discover electricity; he was the first to suggest that lightning was, indeed, electricity. Initially, Franklin and others theorized that electricity was a fluid, and lightning illuminated its flow. The kite experiment presented a leap forward, helping prove that lightning was not a fluid at all - it was simply a huge spark caused by charged electrical forces.

- [About the data](#)
- [About GHRC DAAC](#)

Lightning is still unpredictable and hazardous to experiment with; physicist Georg Wilhelm Richmann died trying to replicate Franklin's kite experiment. Today, however, technology provides safer ways to study lightning, and satellites now track the unruly electrical phenomena in the atmosphere, allowing researchers to learn more about its role in many of Earth's processes. Lightning observations are helping researchers predict severe weather and may help pinpoint where wildfires have ignited. Changes in global lightning patterns may even shed light on changes in Earth's climate.



Lightning strikes near Helsinki, Finland during a 2012 storm. (Courtesy Timo Newton-Syms/Flickr)

Finding the flashes

Ground-based lightning mapping stations have recorded lightning for decades. The stations are often little more than an instrument box the size of a picnic cooler, powered by a single solar panel, and mounted with an antenna to detect passing lightning. “Those produce spectacular imagery of lightning flashes,” said Michael Peterson, a remote sensing scientist at Los Alamos National Laboratory. “But they have very limited range.”

The stations are often placed in rural areas with open fields, but can also be installed in cities on building rooftops. Stations are typically networked in arrays, which detect lightning within a radius of 200 to 300 kilometers (124 to 186 miles). Yet storms frequently sweep outside an array’s range, creating gaps in lightning detection. In addition, arrays exist in only a handful of states, plus Canada, Columbia, Spain, and France. The lack of continuous coverage limited what forecasters could learn about lightning and storm development.

To enable truly global lightning detection, NASA developed space-based lightning-sensing instruments. In 1997, NASA launched the Tropical Rainfall Measuring Mission (TRMM) satellite equipped with a Lightning Imaging Sensor (LIS). The TRMM LIS tracked lightning in a narrow band around the equator spanning 38 degrees North and South, a range that covered the entire length of the African continent, but missed many Northern Hemisphere countries. Like a powerful camera, LIS captured lightning flashes at about 500 frames per second, permitting researchers to follow the evolution of each flash in detail.

A new identical LIS instrument aboard the International Space Station (ISS) extends the TRMM LIS record and increases the swath of observations to 54 degrees North and South, which includes the contiguous United States and more of Europe and Asia. TRMM and ISS LIS standard, science quality data are both available at NASA’s Global Hydrology Resource Center (GHRC) Distributed Active Archive Center (DAAC). Near-real time ISS LIS data are available through NASA’s Land, Atmosphere Near real-time Capability for EOS (LANCE).



Lightning flashes can be complex, such as when they break out into multiple branches. (Courtesy AR Nature Gal/Flickr)

Sensing storm stages

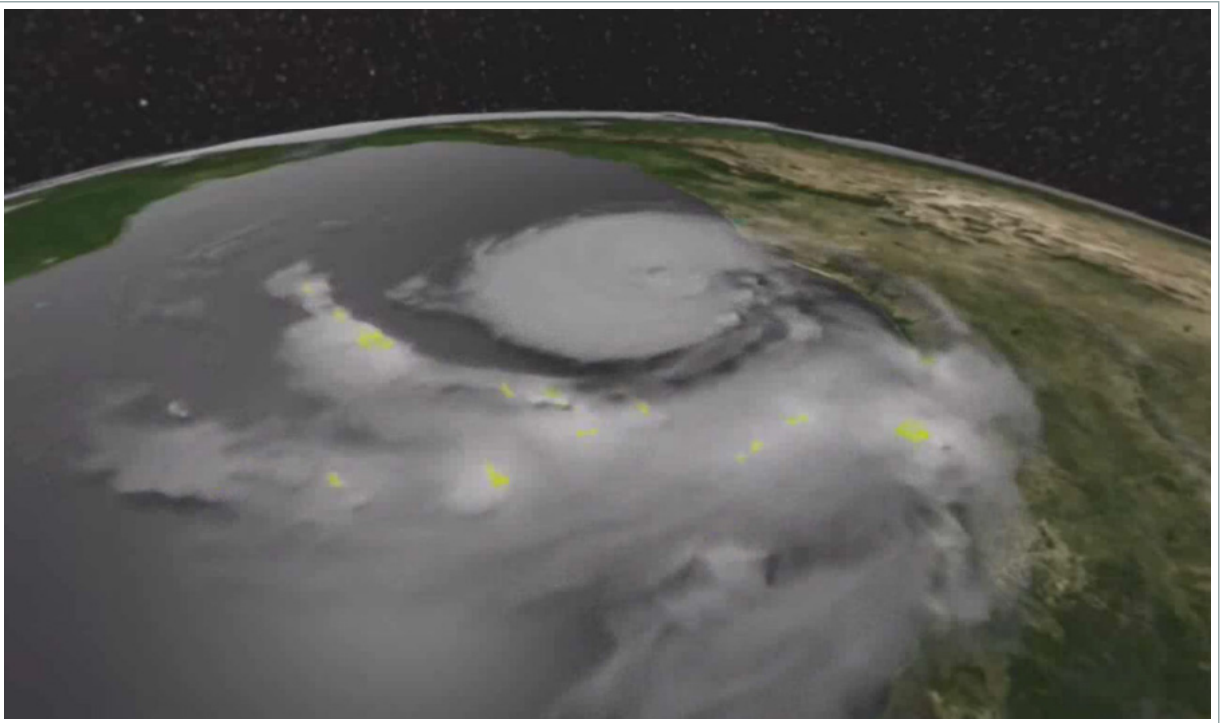
Global views from space reveal that many lightning flashes are far more than a single bolt crackling across the sky. “People tend to think of lightning as a point on a map,” Peterson said. “But the location of the strike hitting the ground only represents a small portion of the larger and complex flash structure. A lightning flash might span hundreds of miles from one point to the other end of it.”

“It’s challenging our view of lightning,” Peterson said. “Back in the olden days, the American Meteorological Society defined a lightning flash as just a series of electrical discharges within a very specific point in time and space.” Now, satellite sensors catch extreme flashes that span surprising distances. “A flash might begin close to Baltimore and might terminate in New York City, affecting four different states along its path,” Peterson said. In another case, Peterson and his colleagues mapped a bolt with 234 visible branches.

These long and often long-lasting extreme flashes can illuminate how storms intensify. “By looking at how the lightning is changing, we can also get a sense for how the storm is changing,” Peterson said. During initial stages when storms are smaller, lightning tends to occur as single flashes that light up a large portion of the surrounding sky. This is because light can more easily escape from smaller storm cells. As storms intensify and increase in size, flashes become more complex, and when viewed from the ground, burgeoning storm clouds may dim or shield parts of the lightning flashes.

“You get a transition from these large and stationary types of lightning flashes, which look like LEDs blinking in the middle of the cloud, to these horizontally extensive long lightning flashes,” Peterson said. Satellite instruments can see through clouds to track how flashes become extreme, developing not just vertically, from cloud to ground, but horizontally, from cloud to cloud.

Monitoring this transition could help forecast severe storms. Peterson and other researchers use a combination of LIS, lightning mapping arrays, and other remote sensors, like the Geostationary Lightning Mapper (GLM), to better understand how lightning and storms develop and evolve together. In fact, researchers have used ISS LIS lightning data to watch squalls strengthen into storms as they sweep across the United States, and followed Hurricane Harvey as it intensified over the Gulf of Mexico in August 2017.



Lightning characteristics can help researchers monitor storm development. This image from the Lightning Imaging Sensor deployed on the International Space Station shows lightning (yellow pixels) in Hurricane Harvey as it approached the Texas coast in 2017. (Courtesy Michael Peterson)

Window into wildfire starts

Although stormy weather often brings much needed rain to arid regions, lightning carries the risk of wildfire. Phil Bitzer, a researcher at the University of Alabama in Huntsville, uses LIS to help identify lightning flashes that may have caused fires. "We noticed something peculiar about the flashes we were seeing," Bitzer said. "These were actually flashes with something that we call continuing current." Normally, a lightning flash has a flickering quality, appearing to turn off and on. But these peculiar flashes stayed on for a while longer, exhibiting continuing current.

"With normal lightning, when it strikes a tree, the current doesn't last long enough to initiate a fire," Bitzer said. When continuing current lightning strikes a tree, however, the current remains on long enough to heat a tree to its combustion temperature and erupt in flames. "That's why these peculiar flashes are so important to detect," Bitzer said.

LIS and GLM are especially useful for identifying continuing current flashes. Bitzer and his colleagues hope to develop an operational system to flag continuing current lightning against a backdrop of other meteorological data. With enough warning, scout teams or drones could pinpoint exact locations to monitor for potential fires, making it easier to quench wildfires before they spread.



This photograph of a storm over the Mojave Desert illustrates cloud-to-ground lightning. (Courtesy Jessie Eastland)

Sparking answers and questions

Each storm and lightning flash may even be part of much larger process. Atmospheric electrical current flows all around us in a continuous stream called the global electrical circuit. Lightning helps transfer some electrical energy between the atmosphere and the ground, charging Earth like a battery. LIS and GLM data reveal places that are more lightning prone than others, such as the Congo Basin in Africa and [Venezuela's Lake Maracaibo](#). "Identifying these electrified regions has implications for our understanding of the global electrical circuit, which is the global manifestation of electricity," Peterson said. "It's kind of like the lightning version of weather versus climate."

The lengthening satellite record of lightning offers clues about whether storms and lightning patterns around the globe might be changing. "It's not going to give you a temperature estimate or anything like that," Peterson said. "But if we can do a good job of understanding how the circuit works, we can use that as a climate indicator."

Do researchers expect to see a change in lightning as climate changes? "Early work suggested yes; more recent work says maybe, maybe not. It's an open question," Bitzer said. "But we certainly have the data to at least answer, 'Is lightning changing?'"

Even though researchers do not completely understand all the interactions and potential climate connections, TRMM and ISS LIS have generated a growing lightning time series, which researchers continue to learn from. "There's so much great work that we've been able to do with TRMM LIS over the years," Bitzer said. "It was the first real climatology of worldwide lightning data." Like Benjamin Franklin, lightning researchers are not just thrill seekers or storm chasers—they too hope to harness the power of lightning. But instead of summoning it from the heavens, they can safely watch and learn from high above.



A photograph taken from the International Space Station captures a nighttime lightning flash over the Pacific Ocean. (Courtesy NASA ISS)

For more information

[NASA Global Hydrology Resource Center Distributed Active Archive Center \(GHRC DAAC\)](#)


[NASA Land, Atmosphere Near real-time Capability for EOS \(LANCE\)](#)


[NASA Lightning Imaging Sensor on the International Space Station \(ISS LIS\)](#) 


[Tropical Rainfall Measuring Mission Lightning Imaging Sensor \(TRMM LIS\)](#) 


[Lightning research at NASA GHRC DAAC](#) 


References

Blakeslee, Richard J. 1998. Lightning Imaging Sensor (LIS) on TRMM Science Data. Dataset available online from the NASA Global Hydrology Center DAAC, Huntsville, AL, U.S.A. [doi:10.5067/LIS/LIS/DATA201](https://doi.org/10.5067/LIS/LIS/DATA201) .

Blakeslee, Richard J. 2017. Non-Quality Controlled Lightning Imaging Sensor (LIS) on International Space Station (ISS) Provisional Science Data. Dataset available online from the NASA Global Hydrology Center DAAC, Huntsville, AL, U.S.A. [doi:10.5067/LIS/ISSLIS/DATA204](https://doi.org/10.5067/LIS/ISSLIS/DATA204) .

Blakeslee, Richard J. 2017. NRT Lightning Imaging Sensor (LIS) on International Space Station (ISS) Provisional Science Data. Dataset available online from the NASA Global Hydrology Center DAAC, Huntsville, AL, U.S.A. [doi:10.5067/LIS/ISSLIS/DATA205](https://doi.org/10.5067/LIS/ISSLIS/DATA205) .

Peterson, M., S. Rudlosky, and W. Deierling. 2017. The evolution and structure of extreme optical lightning flashes. *Journal of Geophysical Research: Atmospheres* 122: 13,370-13,386. [doi: 10.1002/2017JD026855](https://doi.org/10.1002/2017JD026855) .

Yanoviak, S. P., E. M. Gora, J. M. Burchfield, P. M. Bitzer, and M. Detto. 2017. Quantification and identification of lightning damage in tropical forests. *Ecology and Evolution* 7: 5,111-5,122. [doi:10.1002/ece3.3095](https://doi.org/10.1002/ece3.3095) .

Yanoviak, S. P., E. M. Gora, J. Fredley, P. M. Bitzer, R.-M. Muzika, and W. P Carson. 2015. Direct effects of lightning in temperate forests: a review and preliminary survey in a hemlock-hardwood forest of the northern Unites States. *Canadian Journal of Forest Research* 45: 1,258-1,268. doi:10.1139/cjfr-2015-0081 [↗](#).

About the remote sensing data			
Satellite			Tropical Rainfall Measuring Mission (TRMM)
Platform	International Space Station (ISS)	ISS	
Sensor	Lightning Imaging Sensor (LIS)	LIS	LIS
Data sets	NRT Lightning Imaging Sensor (LIS) on International Space Station (ISS) Provisional Science Data ↗	Non-Quality Controlled Lightning Imaging Sensor (LIS) on International Space Station (ISS) Provisional Science Data ↗	Lightning Imaging Sensor (LIS) on TRMM Science Data ↗
Resolution	4 to 8 kilometer	4 to 8 kilometer	3 to 6 kilometer
Parameter	Lightning	Lightning	Lightning
DAACs	NASA Land, Atmosphere Near real-time Capability for EOS (LANCE)	NASA Global Hydrology Resource Center Distributed Active Archive Center (GHRC DAAC)	NASA GHRC DAAC
LANCE ISS LIS data are only stored for seven days and are not archived.			

The blob



Too much warmth and too little wind fueled a massive marine heat wave along the Pacific Coast.

By Laura Naranjo

In 2013, a mysterious pool of warm water developed off of Alaska. This marine heat was so persistent and unusual that it initially defied explanation. The pool lingered in the sub-Arctic Bering Sea and Gulf of Alaska through winter, and then quickly expanded south along the Pacific Coast. By summer of 2014, the heated mass of water stretched from Alaska to Mexico and had been nicknamed “the blob.”

- [About the data](#)
- [About PO.DAAC](#)

As the blob spread, unusually warm waters triggered extended harmful algae blooms. Although such blooms are common, they usually only last a couple of weeks before dissipating. However, the blob fueled longer-lasting and more pervasive blooms, which became toxic to marine life and humans. Higher ocean temperatures also increased warm water algae species, which were less nutritious for marine life.

By the end of 2015, both blob and blooms had shut down much of the Pacific fishing industry and upended the marine food chain. Dead fin whales and sea otters began washing up along the Alaskan coast. Chinook salmon populations in Washington and Oregon plummeted. Hundreds of sea lions starved along California shorelines.

Scientists were left scratching their heads. Why had this warm pool of ocean water spread so far and lingered for so long?



A malnourished sea lion pup is stranded on shore in 2015. A marine heat wave lasting from 2013 to 2016 stranded sea lion pups along the California coast in record numbers. Rescued pups were in a malnourished state by the time they arrived at rehabilitation centers. (Courtesy National Oceanic and Atmospheric Administration Fisheries West Coast)

Whence the warming

One of these scientists, researcher Chelle Gentemann, grew up on the Pacific Coast, where she and her family spent summers fishing for salmon. Now an oceanographer, Gentemann tracks ocean temperatures, and the blob had caught her and her colleagues' attention.

In September 2014, NOAA scientists noted that a buoy off the coast of Newport, Oregon, recorded a seven-degree Celsius (thirteen-degree Fahrenheit) rise in temperature over the course of only one hour. "I know that area really well, and seven degrees is a huge jump," Gentemann said.

Typically, the surface of the ocean follows a daily temperature cycle: warming a bit when the sun is out and cooling again at night. But this spike was well out of normal daily ranges, an ominous sign of how unusually warm the blob was and how quickly it was expanding southward. "The timing of this warm event indicated that it wasn't due to the normal daily heating, but that it really was due to advection [spreading] of a warm patch of water into the area of the buoy," Gentemann said. "And that warm water was from the blob."

Although El Niño conditions were present in 2014, and typically cause warmer oceans and milder winters along the Pacific Coast, researchers ruled it out as a source for the blob. "The El Niño was very weak that year," Gentemann said. "And it has a very distinct signature in how the heat is transferred from the equatorial Pacific up through and along the California coast. And the pattern just didn't match." The blob had formed in the Gulf of Alaska, and spread south. Slight El Niño warming may have magnified some of the temperatures along Mexico and southern California, but it was not behind the blob's persistence or behind the marine die-offs stretching from California to Alaska.



During the Pacific marine heat wave that lasted from 2013 to 2016, hundreds of seabirds starved and died. This common murre was too weak to fly when it was found on the shore of Kodiak Island, Alaska. (Courtesy Robin Corcoran/US Fish and Wildlife Service)

Missing the mixing

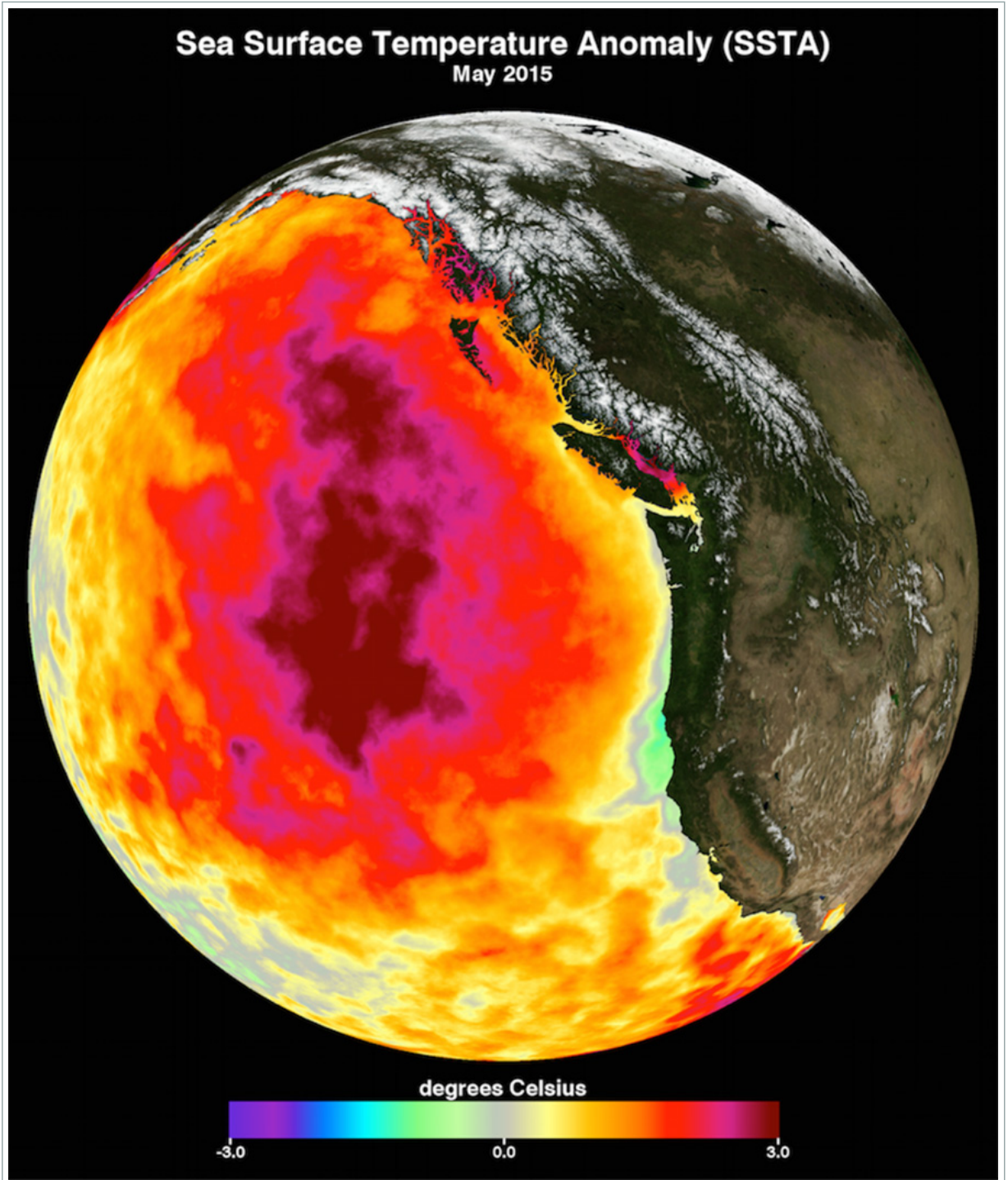
To figure out where this inexplicable warmth was coming from, Gentemann and her colleagues tracked ocean temperatures using an ensemble data set: the Multi-scale Ultra-high Resolution Sea Surface Temperature (MUR SST) Analysis. This ensemble product combines readings from several satellite sensors, and is available from the NASA Physical Oceanography Distributed Active Archive Center.

“Prior to the MUR SST with its one-kilometer resolution, we really didn’t have that glimpse into what was happening along the coast because the satellite data were very spotty,” Gentemann said. Getting a more detailed look at the coastal environment is crucial for understanding ocean mixing. This mixing helps disperse heat from the upper layers of the ocean into deeper waters, while at the same time upwelling cooler, nutrient-rich waters. Nutrients surfaced by upwelling form the basis of the marine food chain. When upwelling is disrupted, so is the coastal food supply.

Because upwelling is fueled in part by temperature, even just a few degrees of abnormal warmth can slow or halt the cycle. But upwelling also depends on winds to help push surface layers away from the coast, providing a horizontal assist to the vertical top-to-bottom upwelling circulation. To complete the emerging picture of a coast in distress, Gentemann incorporated two wind data sets. The Bakun Upwelling Index measures sea level pressure as a proxy for wind stress at the ocean surface, and the European Centre for Medium-Range Weather Forecasts Re-Analysis-Interim Winds product provided wind velocity data.

Gentemann and her colleagues found that prolonged heat from the blob, combined with unusually weak coastal winds, hindered upwelling along much of the Pacific Coast during the marine heat wave. Like the blob, the weakened winds were unusual. Atmospheric rivers normally delivered a steady stream of winds and precipitation from the Pacific. But these rivers were being blocked by a persistent ridge of high pressure in the atmosphere that hunkered over the north Pacific between 2012 and 2015. “It was preventing the winter storms from hitting the West Coast,” Gentemann said. Storms typically usher in windier weather along the coast that help churn the ocean surface and foster upwelling. “There were just no storms. It was just sunny the entire winter,” Gentemann said. “The storms would come up and then they’d hit this ridge and go north.” Fewer storms meant less wind, less

upwelling, and fewer nutrients for fish, but ripe conditions for extensive algal blooms. This devastating combination starved whales, sea lions, fish, and a host of marine life. Even seabirds like common murre, which feed on fish and mollusks that flourish in typically cold coastal waters, starved along coasts from Alaska to California.



This data image shows the monthly average sea surface temperature for May 2015. Between 2013 and 2016, a large mass of unusually warm ocean water--nicknamed the blob--dominated the North Pacific, indicated here by red, pink, and yellow colors signifying temperatures as much as three degrees Celsius (five degrees Fahrenheit) higher than average. Data are from the NASA Multi-scale Ultra-high Resolution Sea Surface Temperature (MUR SST) Analysis product. (Courtesy NASA Physical Oceanography Distributed Active Archive Center)

Ominous impacts

Scientists do not yet know what caused the unprecedented atmospheric ridge, or why it persisted so long. Some research hints that overall ocean warming stimulated this response. Other research indicates the opposite, that the ridge caused the blob to form, and a persistent feedback compounded the multi-year endurance of both blob and ridge. Yet other studies implicate changes in Arctic sea ice that cause shifts in global atmospheric patterns.

The atmospheric ridge dissipated in 2015, and the blob finally subsided in early 2016, but marine animals—and the many coastal industries that depend on them—will take much longer to return to normal. Some species may take years to recover. Waylaid by the disaster, some fisheries and canneries shuttered their doors.

Although marine heat waves are nothing new, and have occurred in seas and oceans around the globe, climate change may amplify them. “You would in some sense expect them to be more common, because in general, the Earth is warming,” Gentemann said. “But whether or not you get these extreme events, whether those increase in frequency, as well, is a question a lot of scientists are asking right now.”

Gentemann and her colleagues plan to continue tracking sea surface temperatures using the MUR SST product. Not only can they monitor future marine heat waves, but develop better ways to characterize them and understand how they impact coastal regions. “Is it a ten-day warming, or is it a two-year warming?” Gentemann asked. “These high-resolution analyses are critical to being able to understand what is going on directly at our coasts, because it’s such a dynamic region.”



The blob of warm water that spread from Alaska to Mexico between 2013 and 2016 devastated many commonly-fished marine species, including Coho salmon. (Courtesy US Bureau of Land Management)

For more information


[NASA Physical Oceanography Distributed Active Archive Center \(PO.DAAC\)](#)

References

Gentemann, C. L., M. R. Fewing, and M. Garcia-Reyes. 2017. Satellite sea surface temperatures along the West Coast of the United States during the 2014-2016 northeast Pacific marine heat wave. *Geophysical Research Letters* 44: 312-319. [doi:10.1002/2016GL071039](https://doi.org/10.1002/2016GL071039)

JPL MUR MEaSURES Project. 2010. Multi-scale Ultra-high Resolution (MUR) Sea Surface Temperature (SST) Analysis (MUR SST) v4.0. PO.DAAC, CA, USA. https://podaac.jpl.nasa.gov/Multi-scale_Ultra-high_Resolution_MUR-SST

About the remote sensing data

About the remote sensing data	
Satellites	Various
Sensors	Moderate Resolution Imaging Spectroradiometer (MODIS) Advanced Very High Resolution Radiometer (AVHRR) Advanced Microwave Scanning Radiometer-EOS (AMSR-E) Advanced Microwave Scanning Radiometer 2 (AMSR2) WindSat Buoys/ships
Data set	Multi-scale Ultra-high Resolution (MUR) Sea Surface Temperature (SST) Analysis (MUR SST) v4.0 
Resolution	1 kilometer
Parameter	Sea surface temperature
DAAC	NASA Physical Oceanography Distributed Active Archive Center (PO.DAAC)

Tracking survival among Idaho's mule deer



Satellite sensing of summer plants and winter snow helps biologists predict mule deer populations.

By Laura Naranjo

During the winter of 2016 to 2017, storm after storm blasted Idaho, piling the state's snowpack far above average. Areas that received more than twice the usual amount of snowfall buried plants and bushes, starving wildlife. Only 30 percent of Idaho's mule deer fawns survived, about half the usual number. Across the western United States, brutal winters like this kill vulnerable does and fawns, decreasing the following year's population. Even worse, these drops exacerbate an ongoing decline in mule deer numbers.

- [About the data](#)
- [About LP DAAC](#)
- [About NSIDC DAAC](#)

This decline is troubling, because mule deer are critical to many of the West's biomes. "Mule deer are an indicator of healthy, functioning wild ecosystems," said Mark Hebblewhite, a wildlife biologist at the University of Montana. Traditionally, biologists monitor mule deer by capturing a small number of the animals every year and fitting them with radio collars that track them, sometimes until death. However, that method is expensive and time consuming. Hebblewhite and Mark Hurley, a colleague at the Idaho Department of Fish and Game, wanted to find an easier way.

Biologists in Idaho have been radio collaring and monitoring mule deer for nearly twenty years, and the resulting data suggested fawn survival was key to maintaining mule deer populations. Yet fawn survival remained highly unpredictable. What if the researchers could instead track predictors within the ecosystems themselves? "We started looking for ways of measuring habitat- and weather-derived influences on mule deer in different parts of Idaho," Hebblewhite said, hoping to glean environmental predictors from satellite data. Could distant satellites help them estimate the survival of thousands of tiny fawns?



A mule deer doe and her fawn trudge through deep snow in Idaho. (Courtesy Idaho Department of Fish and Game)

Fragile fawns

Named for their large, mule-like ears, mule deer inhabit unforgiving environments, ranging from the high deserts of Mexico to rugged alpine peaks in the Yukon. Although mule deer will eat grass, they mostly browse, biting the leaves off of trees and shrubs, and nibbling flowers and leafy plants. "In most of the semi-arid and western United States, mule deer are the dominant large herbivore," Hebblewhite said. As they roam and feed, mule deer leave behind seed-filled droppings that replenish native forests and grasslands, strengthening native ecosystems. In turn, mule deer are preyed on by mountain lions, bears, wolves, coyotes, and even humans, feeding carnivores further up the food chain.

In Idaho, even during the best of years, mule deer race against time to fatten up for winter. "They try to gain a lot of fat during the summer and fall to make it through the winter," Hurley said. During harsh winters, deer resort to nipping lichen from rock faces or chewing bark off trees. Otherwise, adult deer survive the winter by living off their accumulated fat reserves. Fawns do not have that luxury.

Fawns born in early summer must eat enough to triple in size before winter. But this does not give them enough time to produce adequate fat reserves. "They're always going into winter in substandard conditions," Hurley said. The quantity and quality of what mule deer eat is only one factor; severe winter weather introduces another complication. Although fawns are weaned by fall, they remain with their mother throughout the winter, learning to find food. Long, snowy winters deplete an adult mule deer's fat reserves; slogging through belly-deep snowpack month after month can starve fawns lacking those reserves.



Even the high deserts of Arizona experience winter, and mule deer here often feed on evergreen juniper trees that poke above the snowpack. (Courtesy Grand Canyon National Park)

Finding the predictors

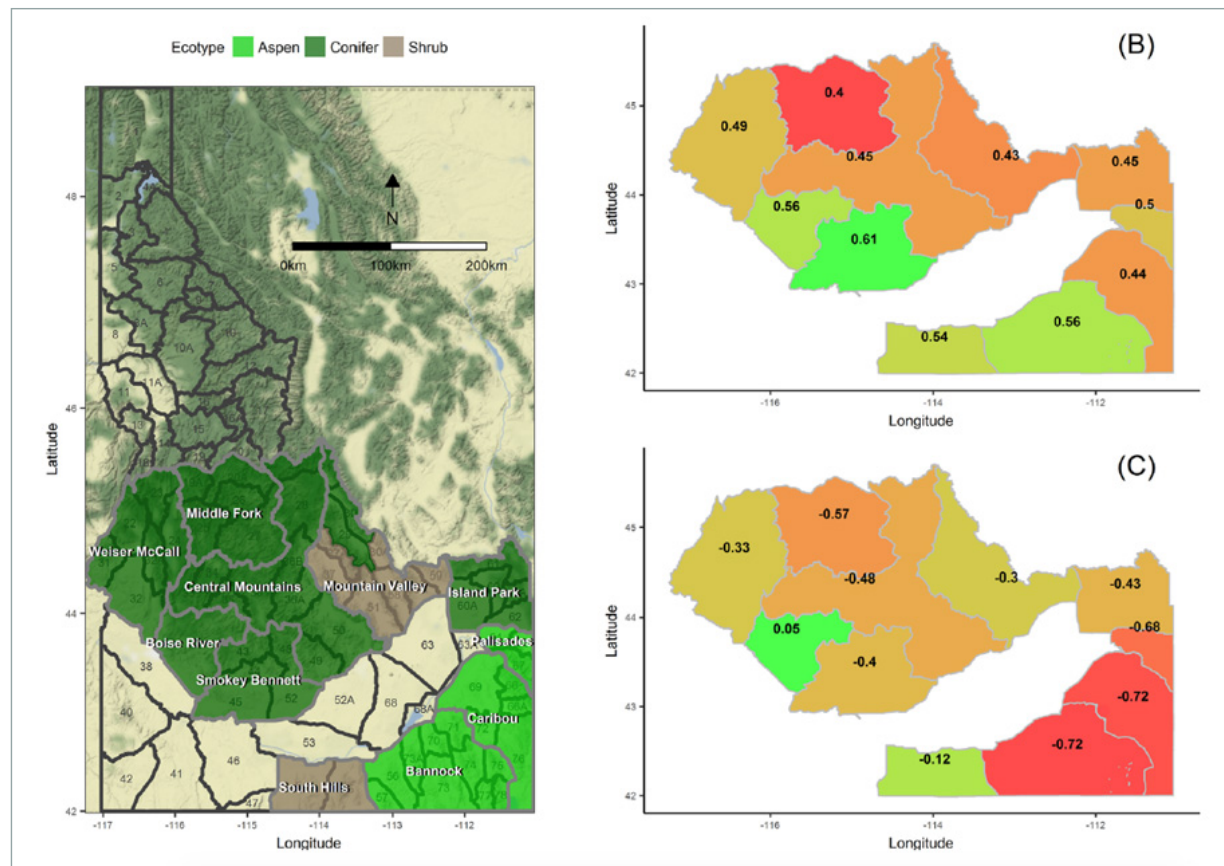
Between 2003 and 2013, biologists working with the Idaho Department of Fish and Game radio collared and tracked 2,529 fawns, recording survivals and deaths across central and southern Idaho. The geographic range covered three major climatic ecotypes that mule deer inhabit: conifer, aspen, and shrub-steppe. With fawn data in hand, the team gathered various vegetation and snow data to see if any stood out as factors for survival. “It was our search for the best predictors,” Hurley said. “What really is influencing fawn survival?”

Because the quality of summer and fall forage matters for deer survival, the researchers relied on a satellite sensor that can measure annual vegetation growth, providing a proxy for ideal deer habitat. Launched in 1999 on NASA's Terra satellite, the Moderate Resolution Imaging Spectroradiometer (MODIS) instrument accrued a time series of data matching the radio collar time span. These vegetation data at 250-meter resolution, spanning March 15 through November 15 annually, captured each growing season from the first tender buds of spring through the last yellowing leaves of autumn.

For winter snow conditions, the researchers encountered a challenge. “These deer live in fairly steep country,” Hurley said. “You have quite an elevation change within a one-kilometer pixel.” Snow does not blanket a mountain range uniformly, and snow cover varies dramatically from peak to valley, or from one mountain face to another. Lower-resolution data could not map such distinctions. The team tried several products before finding success with the finer resolution of MODIS 500-meter snow cover data, which captured subtler differences in terrain and snowpack.

The team developed eleven different models, combining the radio collar record and satellite data. To indicate winter severity, they focused on snow cover and snow depth in early winter, midwinter, and late winter. Spring

and fall vegetation quality represented fat reserves heading into winter. Some of the models were simple, including only a few variables, while others included up to seven. After analysis, Hurley and his colleagues discovered the simplest models were often the most accurate. Early winter severity combined with fall forage quality seemed to best predict fawn survival. Hebblewhite said, “Our models stunned us at how well they predicted.” Better yet, the team included early prediction models, which revealed these predictors held true even if the model only included data for early winter. Hurley said, “That seems to be a very nice predictor of what survival is going to be through the rest of the winter.”



Map A illustrates the three most common mule deer habitats: conifer, aspen, and shrub-steppe. Map A also shows Game Management Units (GMUs) in black boundaries and larger-scale Population Management Units (PMUs) in grey boundaries. Map B shows estimated overwinter survival of mule deer fawns, and map C shows how much snow cover affected fawn survival. For maps B and C, green colors indicate winters during which mule deer are more likely to survive and orange to red colors indicate winters the deer are less likely to survive. Normalized Difference Vegetation Index and snow data are from the Moderate Resolution Imaging Spectroradiometer (MODIS) sensor aboard the NASA Terra satellite. (Courtesy M. Hurley, et al., 2017, *The Journal of Wildlife Management*)

Better models, better management

For the models to be useful, they had to be integrated into the Idaho Department of Fish and Game’s management process. Across the West, states rely on hunting to help manage and conserve wildlife. The risks of overharvesting species are severe, so getting these models to game managers was critical, and timing was the catch. The Idaho department releases each year’s autumn hunt quotas in March, even though traditional radio-collared population tracking is not complete until summer. Incorporating the early prediction models meant managers could set harvest limits for the upcoming year as early as January, eliminating that lag time. Better herd management boosts a state’s bottom line, since most states fund their conservation programs by selling hunting licenses. During 2016 fiscal year, Idaho collected nearly \$40 million dollars in hunting and fishing license sales. Healthy, well-managed species mean more revenue.

Hurley and Hebblewhite worked with colleagues Paul Lukacs and Josh Nowak at the University of Montana in Missoula to develop an application to automate and run the models. The resulting application, which the team named PopR, allows game managers to project future mule deer populations. “They can download the NASA data,

prepare the variables, and run the survival prediction models within this PopR software,” Hurley said. By adjusting snowpack, fall forage, or harvest quotas, game managers can see whether the number of mule deer will grow or decrease.

Collaborating with local biologists was key to PopR’s success. Hebblewhite said, “We achieved buy-in through face-to-face workshops and training sessions and lots of one-on-one meetings.” Creating a portable tool that displays population projections in real time also made it much easier for game managers to explain their decision-making process to the public. According to Hebblewhite, an Idaho manager can bring up department data that are being analyzed with the models and pull in MODIS data distributed by NASA’s Land Processes Distributed Active Archive Center (LP DAAC) and National Snow and Ice Data Center (NSIDC) DAAC. “They can display it right on their phone in public fish and game commission meetings,” he said.

Prior to the 2016 to 2017 winter, Idaho’s mule deer populations were on the rise, which helped cushion that winter’s fawn deaths. The Idaho Department of Fish and Game used PopR for the first time in 2016 to track mule deer populations and set hunt quotas. For the 2017 to 2018 hunting season, game managers reduced the number of mule deer doe licenses in southern and central Idaho game units to help the herds rebound. PopR is designed to be portable and flexible, and is also being used by South Dakota and Montana to manage game. The researchers expect more states to adopt PopR in the future. “That’s why PopR is pretty exciting,” Hurley said. “It’s our charge to understand population dynamics. PopR allows us to answer those ecology questions beyond just management.”



Mule deer are named for their large, mule-like ears. These mule deer are feeding along the sage flats in southern Idaho. (Courtesy Jess Johnson/Flickr)

For more information

[NASA Land Processes Distributed Active Archive Center \(LP DAAC\)](#)


[NASA National Snow and Ice Data Center DAAC \(NSIDC DAAC\)](#)


[NASA Moderate Resolution Imaging Spectroradiometer \(MODIS\)](#) 


[Idaho Department of Fish and Game](#) 


[W. A. Franke College of Forestry and Conservation, University of Montana](#) 


References


Hall, D. K. and G. A. Riggs. 2006. MODIS/Terra Snow Cover 8-Day L3 Global 500m Grid, Version 5, Boulder, CO, USA. NASA National Snow and Ice Data Center Distributed Active Archive Center. [doi:10.5067/C574UGKQU1T](https://doi.org/10.5067/C574UGKQU1T) .




Hebblewhite, M., M. Hurley, P. Lukacs, and J. Nowak. In press. Predicting mule deer (*Odocoileus hemionus*) harvest in real-time: Integrating satellite remote-sensing measures of forage quality and climate in Idaho. In *Satellite Remote Sensing for Conservation Action* , eds. A. K. Leidner and G. M. Buchanan. Cambridge: Cambridge University Press.

Hurley, M. A., M. Hebblewhite, P. M. Lukacs, J. J. Nowak, J.-M. Gaillard, and C. Bonenfant. 2017. Regional-scale models for predicting overwinter survival of juvenile ungulates. *The Journal of Wildlife Management* 81(3): 364-378. [doi:10.1002/jwmg.21211](https://doi.org/10.1002/jwmg.21211) .

Didan, K. MOD13Q1 MODIS/Terra Vegetation Indices 16-Day L3 Global 250m SIN Grid V005. 2015, distributed by NASA EOSDIS Land Processes DAAC, USGS Earth Resources Observation and Science (EROS) Center, Sioux Falls, SD. https://lpdaac.usgs.gov/main_menu/dataset_discovery/modis/modis_archived_documentation. .

National Operational Hydrologic Remote Sensing Center. 2004. Snow Data Assimilation System (SNODAS) Data Products at NSIDC, Version 1. Boulder, CO, USA. NSIDC: National Snow and Ice Data Center. <https://nsidc.org/data/g02158> .

Nowak, J. J., P. M. Lukacs, M. A. Hurley, A. J. Lindbloom, K. A. Robling, J. A. Gude, and H. Robinson. 2017. Customized software to streamline routine analyses for wildlife management. *Wildlife Society Bulletin*. [doi:10.1002/wsb.841](https://doi.org/10.1002/wsb.841) .

About the remote sensing data			
Satellite	Terra	Terra	
Sensor	Moderate Resolution Imaging Spectroradiometer (MODIS)	MODIS	
Data sets	MOD13Q1 MODIS/Terra Vegetation Indices 16-Day L3 Global 250m SIN Grid V005 	MOD10A2 MODIS/Terra Snow Cover 8-Day L3 Global 500 m Grid, Version 5 	Snow Data and Assimilation System (SNODAS) Data Products at NSIDC, Version 1 
Resolution	250 meter	500 meter	30 arc seconds
Parameters	Normalized Difference Vegetation Index (NDVI)	Snow cover extent	Snow cover, snow water equivalent
DAACs	NASA Land Processes Distributed Active Archive Center (LP DAAC)	NASA National Snow and Ice Data Center (NSIDC) DAAC	NASA NSIDC DAAC

Under CATS eyes



Tracking a volcanic plume reaches new heights, faster.

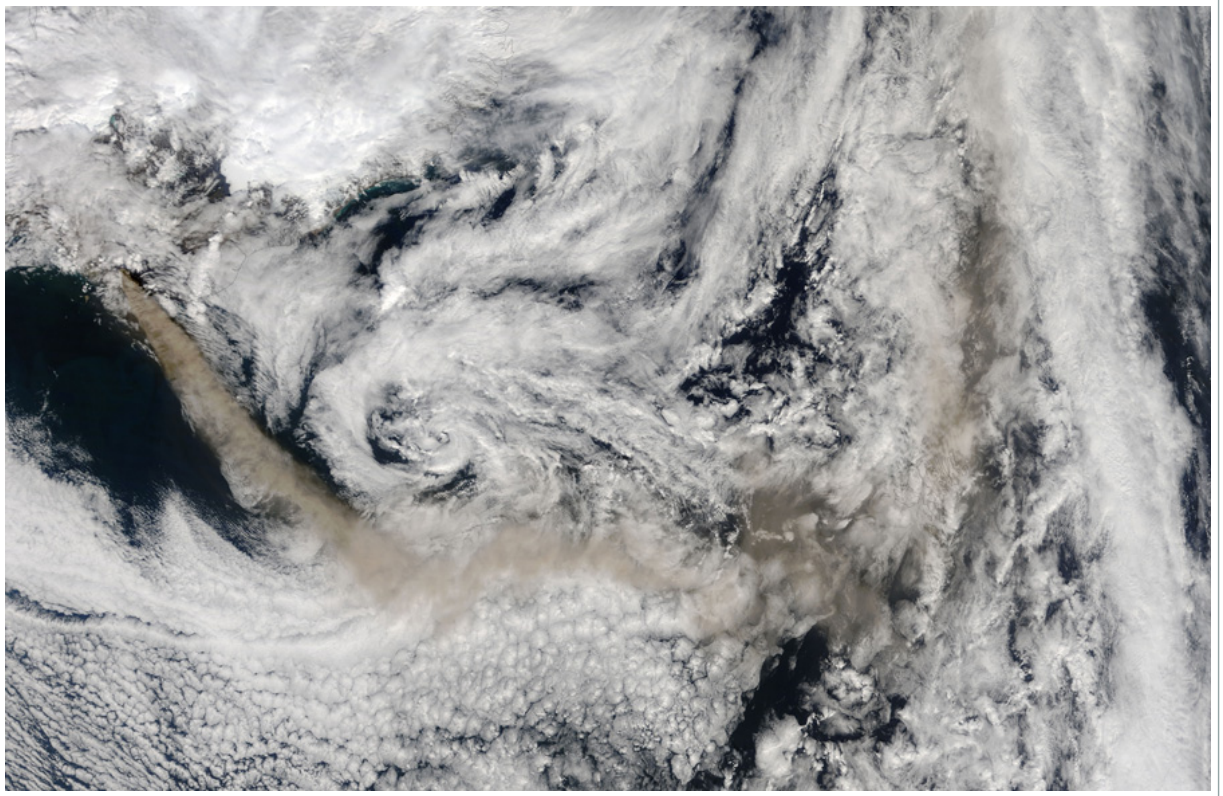
By Agnieszka Gautier

On April 14, 2010, day turned to night when Eyjafjallajökull in Iceland erupted, billowing volcanic ash and sulfur dioxide into the atmosphere. Eight hundred people were evacuated, while hundreds more were confined inside because of the noxious ash fall, which already poisoned nearby farm animals. The plume then drifted across Europe, creating the largest air travel disruption since World War II. Over 100,000 travelers were grounded in eight days. “It was a big headache for the aviation industry, costing billions in canceled flights,” said John Yorks, a research scientist at NASA's Goddard Space Flight Center.

- [About the data](#)
- [About ASDC](#)

Neither a pilot nor weather radar can distinguish a volcanic plume from a regular cloud, with potentially catastrophic results. Ash clouds—or tiny, jagged fragments of pulverized rock and glass—instantly melt within a plane's multiple 1,000-degree Celsius (1,832-degree Fahrenheit) jet engines, coating turbine blades with glass and shutting engines down. Since the 1990s, experts from nine Volcanic Ash Advisory Centers have advised the aviation industry, using a mosaic of data, including satellite data, to map the plumes. Too often, the most comprehensive satellite data have lagged.

Launched in 2015 and operational for 33 months, a small NASA instrument on the International Space Station (ISS) delivered an unexpected bonus—it cut the waiting period for this detailed data. The Cloud-Aerosol Transport System (CATS) project was cheaper than the big missions, but its small sensor accomplished something mighty, and Yorks understood its potential impact.



On May 13, 2010, the Moderate Resolution Imaging Spectroradiometer (MODIS) instrument on the NASA Terra satellite captured Eyjafjallajökull volcano's ash plume mixing with the weather system over the Atlantic Ocean and onto Europe. (Courtesy Rob Gutro/NASA Goddard Space Flight Center)

A dreamer soars

When John Yorks was a little boy, he lay in the yard of his suburban Philly home watching the clouds. Some puffs swirled, other streaks scurried, while still others seemed to stand still. Yorks wondered how is this possible? Why do they move at different speeds? Are they at different heights? He studied these questions through to his PhD, and then arrived at NASA to work on the CATS project. Little did he know that his boyhood wonders would unravel complex problems—like accurately tracking a volcanic plume.

CATS uses Light Detection and Ranging (Lidar), a remote sensing method that measures ranges or variable distance to Earth with a pulsed laser. The pulse's intensity can describe cloud composition, aerosol type and abundance, even the altitudes of these layers.

Prior to satellite lidars, NASA relied on passive sensors, which processed radiation reflected and emitted by Earth's atmosphere. This method could detect aerosol and cloud concentrations but was unable to distinguish heights. For continuous, near-global coverage NASA turned to space. CATS was only the second lidar instrument to make it there. The first was the NASA Cloud-Aerosol Lidar and Infrared Pathfinder Satellite Observations (CALIPSO) satellite, which began tracking smoke from fires, dust storms, and volcanic eruptions in 2006.

CALIPSO's primary mission lasted three years, and since has relied on its backup laser. The next satellite mission with a lidar onboard is scheduled to launch in 2018. Scientists saw CATS as a potential bridge between these two space missions.

Yorks helped a team of engineers at NASA Goddard build CATS with CALIPSO data users in mind. They wanted the data to feel familiar. Unfortunately, CALIPSO data downloading capabilities were slow. It was primarily used for validation, and correcting calculations if the plume was long-lasting, like the 2011 eruption from Puyehue-Cordón Caulle in Chile, which circled the globe three times.

With CATS being on the ISS, Yorks realized data could be downloaded quickly, meaning airlines and communities could be warned within hours of a plume's path. What he needed now was a demonstration.



The shaded area shows an estimation of the Eyjafjallajökull volcano's ash cloud originating in Iceland and spreading over Europe on Apr 15, 2010. The red dot indicates the volcano's location. (Courtesy de.wikinews.org)

The guts within

On December 3, 2015, Sicily's Mount Etna spewed a cloud of volcanic ash and sulfate aerosols into the atmosphere. Though not a big eruption, Etna was good forecasting practice. While Yorks processed the data from CATS, a few scientists down the hall began forecasting the plume's path. They initially did so without any lidar information. Eric Hughes, a graduate student at the University of Maryland, assisted. He said, "Modeling plumes is a really cool transport problem." A plume disperses in air like ink in water. How it moves is a matter of internal, quantity and force, and external components, such as temperatures and winds.

In Mount Etna's case the ash fell out within the first day of eruption, separating from sulfur dioxide (SO_2). SO_2 oxidizes to sulfate aerosols, which can remain as long as three or four years in the atmosphere, cooling the globe by scattering solar radiation. Dust-like, volcanic ash can also be difficult to quantify, whereas SO_2 has a straightforward visible signature within the light spectrum. The team, therefore, focused on SO_2 . Roughly nine hours after the eruption, an ultraviolet spectrometer produced vertical density maps of SO_2 from the Ozone Mapping and Profiler Suite Nadir Mapper (OMPS-NM) on board the NASA-NOAA Suomi National Polar-orbiting Partnership (Suomi-NPP).

Using model winds on a super computer, the scientists locked onto SO₂ particles within the plume, and traced them back in time to the eruption. From many possible backward paths, they chose the one that arrived closest to Mount Etna, and used its lock-in altitude to see into the future. Its estimated altitude was 7 to 12 kilometers (4 to 8 miles) high within the atmosphere. “Most of the time, we can get the forecast fairly right, but in this case we really got it pretty wrong,” Hughes said. Something went wrong with the model, but Hughes was not sure what.

Then Yorks appeared with the CATS data. And because the CATS data were processed similarly to CALIPSO data, Hughes could jump right in. He wanted to know what happened. According to CATS, the plume height should have been at 11.5 to 13.5 kilometers (7.1 to 8.4 miles). Though not a huge difference, it greatly affected the plume trajectory. “If you don’t know that altitude, it’s really hard to model,” Hughes said.

Volcanoes can erupt as high as 45 kilometers (28 miles), penetrating the stratosphere. Rain clears ash and aerosols in the troposphere, but in the stratosphere it disperses slower. The original trajectory had the entire plume in the jet stream, where fast winds blow into Asia. Instead, the Mount Etna eruption cloud lingered. Hughes said, “When you get the altitude wrong, you’re placed in the wrong part of the atmosphere, and because winds vary with altitude, if you get that wrong, the winds push you in the wrong direction.” The CATS altitude placed part of the plume in the jet stream and part above, traveling more gradually eastward.



Lava flows on the upper east flank of Mount Etna in Sicily, Italy in 2006. (Courtesy Robin Campion/Imaggeo)

Timing is everything

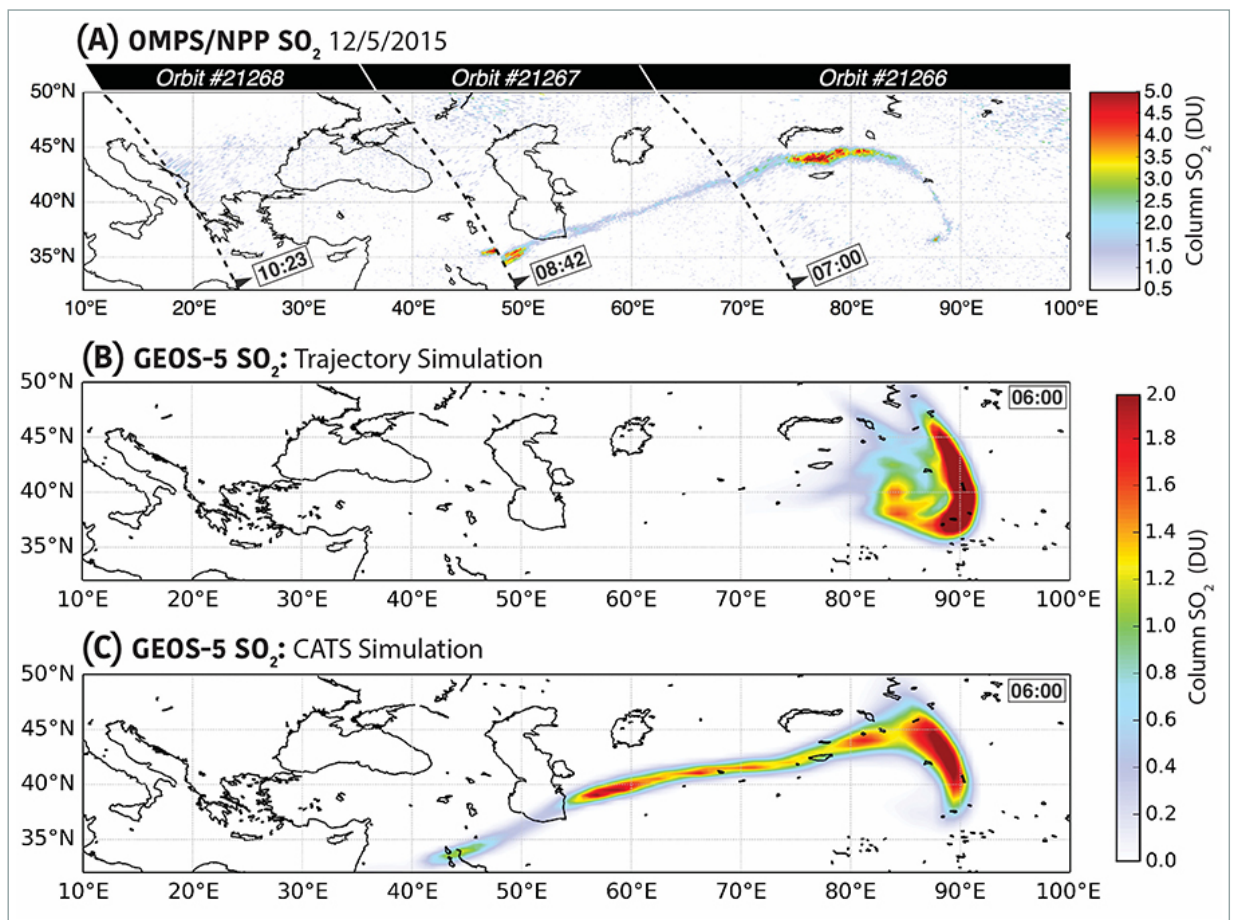
The team would have been able to correct their trajectory using CALIPSO data, but CATS data could be downloaded within minutes and then processed within a three- to six-hour latency. Hughes realized that CATS data could be used to forecast in near real-time. This would be a first. CALIPSO can take three days to process data. Partially, because CALIPSO’s orbit is set up to remap the same point once every 16 days, meaning it has a more comprehensive view of Earth, and, unlike CATS, it maps the polar regions. Though CATS has a narrower view of Earth, it overlaps the areas with more volcanic activity more frequently.

In the future, Hughes hopes for more hands-off plume forecasting for volcanic eruptions. “A lot of this analysis is done by hand,” he said. “We need to move toward plume modeling where CATS is assimilated into the model, and the model corrects the forecasts based on the CATS observations.” With CATS near real-time accessibility, this could become a reality.

CATS increased frequency can be more than a bonus to the aviation industry. CATS provides vertical profile measurements, slices of the atmosphere, that help monitor air quality. “Besides plume monitoring, there is a lot of work being done near the surface. So when you have dust storms or wildfires, we’re using lidar data to improve forecasting those events and how those impact human health,” Yorks said. Abrasive aerosols near the Earth’s surface cause deadly respiratory illness, killing 68,000 people in the United States and 3.3 million people globally.

CATS ceased operations in October 2017, outlasting its six-month requirement by a little more than two years. Now that CALIPSO is relying on its backup lidar, fingers are crossed that it will last until the joint European and Japanese spacecraft, EarthCARE, or Earth Clouds, Aerosols, and Radiation Explorer, becomes operational at some point in 2018. The next NASA mission with a lidar aboard is planned for post 2020. A gap in data and loss of long-scale observation may interrupt computer modeling, critical to understanding the climatological impacts of clouds and aerosols.

Yorks and his team have put together a proposal for a second CATS instrument to fly on the ISS, hoping that this time CATS-2 might catch a massive eruption, so modelers like Hughes and his team could use the data in near-real time to track the next big one—something everyone has been preparing for.



These three map plots compare three different methods of forecasting and tracking a December 5, 2015 sulfur dioxide (SO₂) plume from Mount Etna in Sicily, Italy. Map A shows the sulfur dioxide plume using the Ozone Mapping and Profiler Suite Nadir Mapper (OMPS-NM) on board the NASA-NOAA Suomi National Polar-orbiting Partnership (Suomi-NPP). Map B simulates the plume using altitudes estimated from trajectory paths, and map C uses altitude data from the Cloud Aerosol Transport System (CATS) to correct the simulation. In the bar, DU stands for Dobson units (DU), which is a standard unit of measure for ozone in a column of air. (Courtesy E. J. Hughes, et al., 2016, *Geophysical Research Letters*)

For more information

[NASA Atmospheric Science Data Center \(ASDC\)](#)

[Cloud-Aerosol Lidar and Infrared Pathfinder Satellite Observation \(CALIPSO\)](#)

[Cloud-Aerosol Transport System \(CATS\)](#)

References

Hughes, E. J., J. Yorks, N. A. Krotkov, A. M. da Silva, and M. McGill. 2016. Using CATS near-real-time lidar observations to monitor and constrain volcanic sulfur dioxide (SO₂) forecasts. *Geophysical Research Letters* 43, doi:10.1002/2016GL070119 [↗](#).

McGill, M. 2016. CATS-ISS_L2O_D-M7.1-V1-05kmPro. NASA Atmospheric Science Data Center (ASDC), Hampton, VA, USA. doi:10.5067/iss/cats/l2o_d-m7.1-v1-05_05kmpro [↗](#).

Yorks, J. E., M. J. McGill, S. P. Palm, et al. 2016. An overview of the CATS level 1 processing algorithms and data products. *Geophysical Research Letters* 43, doi:10.1002/2016gl068006 [↗](#).

About the remote sensing data	
Platform	International Space Station
Sensor	The Cloud-Aerosol Transport System (CATS)
Data set	CATS-ISS_L2O_D-M7.1-V1-05kmPro ↗
Resolution	5 kilometer
Parameters	Layer height, layer thickness, backscatter, optical depth, extinction, depolarization-based discrimination of particle type
DAAC	NASA Atmospheric Science Data Center (ASDC)

Unwelcome enrichment in the Arctic



Microscopic plastics infiltrate Arctic sea ice with unknown consequences for the ecosystem.

By Michon Scott

The Great Pacific Garbage Patch between California and Hawaii might evoke images of a trash heap floating on the ocean, but it consists of particles too small to be seen by the naked eye. Those particles are plastic.

- [About the data](#)
- [About NSIDC DAAC](#)

Fifty years ago, global annual plastic production was less than 50 million tons; in 2015, production was nearly 450 million tons. Every year, between 5 and 14 million tons of plastic reach the ocean, and that is just from coastal regions.

Plastic polymers are molecular chains that repeat the same simple links. Common examples include polyester clothing, nylon toothbrushes, polycarbonate DVDs, and polyethylene shopping bags. Besides everyday conveniences, plastics such as inflatable life vests and single-use medical devices save lives. Plastics are inexpensive, lightweight, and durable, but their durability poses a problem because they take several hundred years to decompose. Scientists now wonder about the effects of plastics on wildlife and human health.

In the ocean, wind, waves, temperature swings, and sunlight break plastics into microscopic bits. In 2004, marine ecologist Richard Thompson coined a term for these particles: microplastics. Anything smaller than five millimeters (about a fifth of an inch) is considered a microplastic, but microplastics can get much smaller—down to a fraction of the width of a human hair. Even biodegradable plastics leave microplastics behind, and microplastics reach locations as remote as the Arctic.



A plastic particle smaller than five millimeters (about a fifth of an inch) is defined as a microplastic, but many microplastics are too small to be seen with the naked eye. (Courtesy National Oceanic and Atmospheric Administration)

Small size, big trouble

Ilka Peeken is a senior scientist at the Alfred Wegener Institute (AWI) in Bremerhaven, Germany. She originally trained as a phytoplankton ecologist, but switched her focus to the Arctic and the threats posed to it by climate change. "A lot of people don't know this, but sea ice has its own ecosystem. You have tiny algae, worms, and copepods that live in the sea ice and depend on that habitat for food. The organisms living in the sea ice are a big source of food for the higher levels in the polar food chain," she said. Plastic has now been found in this habitat. "Plastic particles are very tiny, and the organisms can't differentiate between plastic and food they should be eating."

Ingested microplastics may leave animals feeling full while offering no nutrition. The particles may obstruct diminutive digestive tracts. Particles inside smaller organisms can be ingested by larger organisms. Peeken said, "But it gets worse because the next step is nanoplastics."

The smallest plastic particles are best measured in microns and nanometers. A millimeter is a thousandth of a meter, a micron is a thousandth of a millimeter, and a nanometer is a thousandth of a micron. For reference, a human hair is somewhere around 50 to 75 microns in diameter. What constitutes a nanoplastic is still debated, but is probably anything less than a micron across, and getting eaten and excreted by some animals can push plastics from one category into another. Passing through a small gut might break particles with a diameter of 31.5 microns down to a single micron across.

Peeken explained what is so scary about these tiniest plastics. "They're able to penetrate cells," she said.

Geir Wing Gabrielsen of the Norwegian Polar Institute echoed Peeken's concerns, saying, "Nanoplastics embedded in phytoplankton get eaten by zooplankton and then by fish. Those particles are getting into the fish's blood, passing through the blood-brain barrier, and affecting behavior." Research has already shown nanoplastic-

induced mortality in small crustaceans, and brain infiltration in fish. Other effects remain poorly understood. What is no longer mysterious is how widespread microplastics have become in global oceans.

Plastic is everywhere.



Nicknamed the water flea, *Daphnia magna* is a tiny crustacean that frequents freshwater environments. Research has indicated that nanoplastic particles can be fatal to these animals. (Courtesy Dieter Ebert/Wikimedia)

Cores of the problem

Microplastics in ocean water end up in sea ice when that water freezes. Peeken and her colleagues designed a study to identify the extent to which microplastics have penetrated Arctic sea ice. She explained that counting microplastics in sea ice offers some advantages over studying microplastics in the water column. "If you do water sampling, you have to make sure you don't contaminate your samples," she said. "In the lab, it's easier to control the temperature and keep dirt out of the air. Then you can look for what is in the ice."

In June 2014, and June and August 2015, the German icebreaker *Polarstern* collected ice cores from five locations. The expeditions drilled cores in sea ice in Fram Strait, north of Svalbard, and in the Nansen Basin. One of the locations in Fram Strait was from landlocked ice; the others were from drifting ice. Back at the lab, researchers cleaned the cores from the outside then let them melt. Next, they filtered the water and subjected the particles to infrared radiation. "Once you bombard each particle, it has a certain absorption or reflection, and that allows you to identify the optical fingerprint of each type of microplastic. It's different for paint particles versus fishing gear particles," Peeken said.

Peeken's team found up to 12,000 particles per liter of sea ice—two to three orders of magnitude higher than the findings of a previous study that relied more on visual inspection. Most of the microplastics Peeken's team found were smaller than 50 microns across, and the infrared microscope could detect particles as little as 11 microns. That was not down to the level of nanoplastics, but it was a more in-depth sample than in the previous study.

Peeken and her colleagues were surprised at the quantity of microplastics. “We found huge numbers compared to what is in the water column,” she said. Sea ice accumulates more than its fair share of microplastics, a process known as enrichment.



Researchers on the German research icebreaker *Polarstern* collected multiple sea ice cores in June 2014, and June and August 2015 to assess microplastic concentrations. (Courtesy Stefanie Arndt/Alfred Wegener Institute)

Retracing steps

The ice cores were illuminating, but they only told part of the story. Sea ice does not circulate as quickly as seawater, but it does travel. All the ice cores Peeken’s team examined were collected along the Transpolar Drift, part of a larger circulation pattern in the Arctic. Except for the landlocked ice core, the cores did not form where they were extracted—different core sections came from different parts of the Arctic Ocean.

To figure out where the ice cores were at various stages in their formation, the team used multiple data sets. “We use sea ice motion to find the microplastic source areas,” said Thomas Krumpfen, one of Peeken’s coauthors and a fellow senior scientist at AWI. One data set that helped the team backtrack the microplastics’ journeys was the Polar Pathfinder Daily 25 km EASE-Grid Sea Ice Motion Vectors, available from NASA’s National Snow and Ice Data Center (NSIDC) Distributed Active Archive Center (DAAC). Drawing from a range of buoy and satellite observations, these data provide monthly, weekly, and daily sea ice motion and velocity. By identifying ice features in separate satellite images, and measuring the change in a feature’s location and the time difference between the images, researchers can estimate ice movement. The time series runs from October 1978 through February 2017. Krumpfen wrangled ice locations to follow sea ice movement during the Northern Hemisphere summers. “Even a low-resolution data set provides an approximation of the ice source,” he said. “It enables us to link observations in the field with ice movement observed by satellite.”

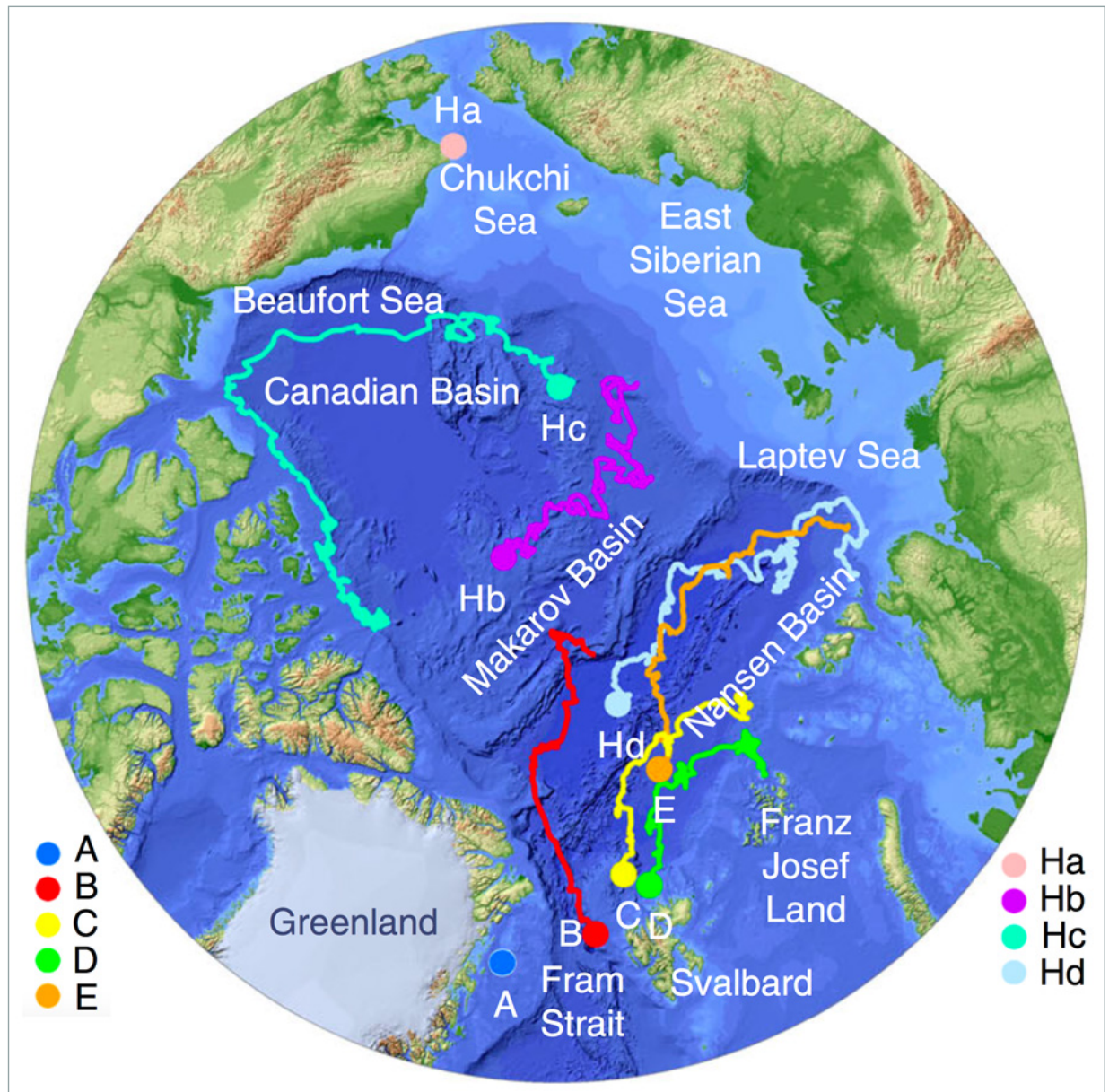
Movement through the Arctic is complicated, but in a rough sense, water enters the Arctic from the Pacific, traveling through the Bering Strait. Water and ice exit the Arctic via the Fram Strait east of Greenland. NSIDC DAAC sea ice data sets enable researchers to better estimate ice location at a particular time. Combining ice core samples and backtracked ice movement enabled the researchers to identify microplastic sources.

“You can envision the ice formation depending on where the ice travels,” Peeken said. “We found extremely high polyethylene in the central Arctic.” These are plastics used in bags and packing material, and the most likely

source is the Great Pacific Garbage Patch. "What we totally didn't expect was to have such a huge variability with the polymer types," she said. Instead, the team found over a dozen different plastic polymer types, including polymers linked to paint and nylon, likely originating from sources in the Arctic, where transport and fishing are on the rise. Increased human presence is becoming more apparent in the Arctic Ocean. Already modeling studies suggest another garbage patch may be forming in the Barents Sea north of Siberia.

Toxicology specialist Gabrielsen was not involved in Peeken's study, but he was as surprised as Peeken at the high numbers of nanoplastic particles, especially in the Fram Strait. As the Arctic's exit ramp, the Fram Strait is the conduit for nearly all the plastic contamination in Arctic sea ice. He now wonders how much plastic animals living in and on the ice are consuming. "It's something we really need to clarify," he said.

Peeken hopes to better understand why nano- and microplastics concentrate more in sea ice than in sea water. Because most of the Arctic food chain in some way depends on sea ice, plastic enrichment in the ice leads to plastic enrichment in the food chain. Meanwhile, Krumpen anticipates using NSIDC DAAC data more often to understand ice transport in general. But Peeken and Krumpen are both sobered by the findings of this study. "There's basically no place on Earth anymore where you don't find microplastics in the ocean," said Peeken. "I think that's important for people to know. Otherwise they don't change their behavior."



This ice-core location map shows the reconstructed sea ice movement for cores collected by the *Polarstern* crew in 2014 and 2015 (A through E), and cores collected by earlier expeditions, in 2005 and 2010 (Ha through Hd). Cores A and Ha came from sea ice holding fast to a shoreline, but other cores came from drifting sea ice. Ice velocity and ice motion data

helped the researchers reconstruct ice motion from the core samples. (Courtesy I. Peeken, et al., 2018, *Nature Communications*)

For more information

[NASA National Snow and Ice Data Center \(NSIDC\) Distributed Active Archive Center \(DAAC\)](#)

[NASA Aqua Earth-Observing Satellite Mission](#)

[Advanced Microwave Scanning Radiometer for EOS \(AMSR-E\)](#)

[Advanced Very High Resolution Radiometer \(AVHRR\)](#)

[SMMR, SSM/I, and SSMIS Sensors](#)

References

Alfred Wegener Institute. [AWI researchers measure a record concentration of microplastic in arctic sea ice](#). Accessed August 27, 2018.

Bluhm, B. A., H. Hop, M. Vihtakari, R. Gradinger, K. Iken, I. A., Melnikov, and J. E. Søreide. 2018. Sea ice meiofauna distribution on local to pan-Arctic scales. *Ecology and Evolution* 8(4). doi:10.1002/ece3.3797

Dawson, A. L., S. Kawaguchi, C. K. King, K. A. Townsend, R. King, W. M. Huston, and S.M. Bengtson Nash. 2018. Turning microplastics into nanoplastics through digestive fragmentation by Antarctic krill. *Nature Communications* 9: 1001. doi:10.1038/s41467-018-03465-9

Gigault, J., A. ter Halle, M. Baudrimont, P.-Y. Pascal, F. Gauffree, T.-L. Phi, H. El Hadri, B. Grassl, S. Reynaud. 2018. Current opinion: What is a nanoplastic? *Environmental Pollution* 235: 1,030-1,034. doi:10.1016/j.envpol.2018.01.024

Law, K. L., R. C. Thompson. 2014. Microplastics in the seas. *Science* 345(6193): 144-145. doi:10.1126/science.1254065

NOAA Marine Debris Program. [What we know about plastic marine debris](#). Accessed October 29, 2018.

NOAA National Ocean Service. [The Great Pacific Garbage Patch](#). Accessed August 27, 2018.

Parker, L. 2018. [We made plastic. Now we're drowning in it](#). *National Geographic*. Accessed August 27, 2018.


Peeken, I., S. Primpke, B. Beyer, J. Gütermann, C. Katlein, T. Krumpfen, M. Bergmann, L. Hehemann, and G. Gerdt. 2018. Arctic sea ice is an important temporal sink and means of transport for microplastic. *Nature Communications* 9: 1505. doi:10.1038/s41467-018-03825-5

Thompson, R. C., Y. Olsen, R. P. Mitchell, A. Davis, S. J. Rowland, A. W. G. John, D. McGonigle, A. E. Russell. 2004. Lost at sea: Where is all the plastic? *Science* 304(5672): 838. doi:10.1126/science.1094559

Tschudi, M., C. Fowler, J. Maslanik, J. S. Stewart, and W. Meier. 2016. *Polar Pathfinder Daily 25 km EASE-Grid Sea Ice Motion Vectors, Version 3*. Boulder, CO USA. NASA National Snow and Ice Data Center Distributed Active Archive Center. doi:10.5067/O57VAIT2AYYY

About the remote sensing data	
Satellites	Aqua; Defense Meteorological Satellite Program F8, F11, F13, and F17; National Oceanic and Atmospheric Administration-9, -11, -12, and -14; Nimbus-7
Platforms	Buoys

About the remote sensing data

Sensors	Advanced Microwave Scanning Radiometer for EOS (AMSR-E) Advanced Very High Resolution Radiometer (AVHRR) Scanning Multichannel Microwave Radiometer (SMMR) Special Sensor Microwave Imager (SSM/I) Special Sensor Microwave Imager/Sounder (SSMIS)
Data set	Polar Pathfinder Daily 25 km EASE-Grid Sea Ice Motion Vectors (NSIDC-0116) 
Resolution	25 kilometer
Parameters	Ice velocity, sea ice motion
DAAC	NASA National Snow and Ice Data Center (NSIDC) Distributed Active Archive Center (DAAC)

Mapping stormwater runoff in Southern California helps keep toxins at bay.

By Agnieszka Gautier

From the infamous Malibu to the quirky Venice, the beaches near Los Angeles (LA) bring out surfers come rain or shine. But surfers entering the waters during and after rainstorms expose themselves to more than just epic swells. Excessive bacteria in water, including fecal coliforms such as *E. coli* and *Enterococci*, are associated with more than 600,000 gastrointestinal illnesses a year. A local environmental organization called Heal the Bay (HTB) monitors these beaches. They found that surfers are 20 percent more likely to get sick in the region's wet winters compared to its dry summers.

- [About the data](#)
- [About ASF DAAC](#)
- [About OB.DAAC](#)

Stormwater runoff is a major source of ocean pollution in LA and Southern California. The Southern California Bight (SCB), a curved coastline from Point Conception to San Diego, is home to nearly 25 percent of the coastal population in the United States. "We have millions of people surrounded by mountains," said Benjamin Holt, a researcher at NASA's Jet Propulsion Laboratory (JPL) in Pasadena, California. "Anything you can think of that happens to be on the streets, enters the ocean—untreated."

Holt has been keeping an eye on the ocean from high above. The native Californian has collected over two decades worth of satellite images of stormwater runoff into San Pedro and Santa Monica Bays to see how satellites could guide in situ water quality data collection and beach monitoring.

Assessing the impacts of stormwater runoff in coastal oceans commonly relies on sparse beach sampling and from onboard research vessels, but boat operations are costly and rain is sporadic. "Monitoring programs could do a lot more with respect to remote sensing," said Michelle Gierach, another JPL researcher and coauthor of the study. By combining two different satellite sensors that image the ocean differently, Holt and his team hope to focus in situ sampling to the most polluted areas along the SCB coast.



Signs warn against trashing the streets of Los Angeles in Highland Park. (Courtesy waltarrrrr/Flickr)

Untreated and toxic

When the wet season arrives in late autumn in southern California, the reprieve from hot, dry summers is a sure welcome. The runoff, however, is not. Built-up trash and grime on the streets and in parking lots concentrate into the rivers that feed the ocean. Everything from cigarette butts, plastics, petroleum, pesticides, fertilizers, heavy metals, and fecal bacteria finds its way there. And with population increases and impervious surfaces spreading, ocean pollution is rising. "There's so much concrete and asphalt in LA that rain water doesn't go into the ground; it just runs off," Holt said.

The LA river is part of the problem. Today it is more of a storm drain than a river. Once an alluvial river, slithering freely in the lush flood plain of southern California, it now inspires little of nature. In 1938, record-breaking rainfall inundated a third of the city, killing 115 people. The river carved new trenches, shifted nearly a mile in Compton, toppled bridges, and swept homes off the land. With this being the third major flood in 25 years, the US Army Corps of Engineers lowered and widened the river, cementing its banks and bottom for 278 miles. The river was unrecognizable. And it was not alone.

Holt's study observed four rivers entering the San Pedro and Santa Monica Bays: the LA, San Gabriel, and Santa Ana Rivers, and Ballona Creek, with only the latter entering Santa Monica Bay. All these rivers are cemented. When the rains come and the rivers swell, water no longer reabsorbs into the soil, instead pollutants and debris accrue into these channels and out to the ocean.



After a rainstorm, a loader removes trash with high concentrations of plastic at the mouth of the Los Angeles River in Long Beach, California. (Courtesy Bill McDonald, Algalita Foundation/plasticpollution/Flickr)

Party pooper

In the ocean, floating trash, leaves, silt, and other effluents dampen its wave height. Synthetic Aperture Radar (SAR) detects this smoothness, called a surface slick, when its radar sent to Earth bounces back weaker, appearing black in the grey-toned images. Since low winds and oil spills can also reduce wave height, Holt and his team verified whether their SAR plumes from 1992 to 2014 were truly from stormwater runoff with precipitation data. If rainfall exceeded 6 millimeters, they attributed the plumes to runoff.

According to the California Department of Public Health beaches should not exceed 104 colony-forming units/100 milliliters (cfu/ml) of *Enterococci* bacteria. Fecal bacteria in water are not necessarily harmful to humans themselves, but they tend to indicate the presence of pathogens, which can result in diarrhea, intestinal cramping, or skin rashes. Since testing for these pathogens is costly, agencies measure their fecal comrades instead.

Holt only matched two rain events of SAR data with Heal the Bay's four-year beach sampling study, in December 2008 and February 2009. SAR data are patchy. Multiple satellites offer its data, but unfortunately, most do not have regular repeating acquisition schedules since they mainly user-driven, meaning its data coverage is sporadic. This makes it hard to match SAR data with likewise sporadic rainfall in southern California. In either case, the plume examples corresponded well with fecal contamination. Where there was a plume, there was a problem.

"The patterns were quite good," Holt said. Harmful fecal concentrations occur most often within one to two days of rainstorms, but not always. Three rivers flow into San Pedro Bay: the LA, San Gabriel, and Santa Ana Rivers. On December 15, 2008 a deluge began. HTB measured contamination levels at the mouths of three rivers, where the worst bacteria levels are typically detected. Three rivers flow into San Pedro Bay: the LA, San Gabriel, and Santa Ana Rivers. On that first day of the storm, both the Santa Ana and San Gabriel Rivers had safe levels of *Enterococci* bacteria, while the LA River had dangerous levels. According to SAR data, no plume developed near or offshore the Santa Ana, validating the results. On December 17, high levels of bacteria were only detected in Ballona Creek and the Santa Ana River.

SAR data offer fine resolution imagery which is able to capture images close to shore. The suggested key observation from this limited overlapping data sets is that harmful bacteria levels appear to be observed only within the SAR-detected plume extent. For Holt, using SAR data provides a unique capability for agencies concerned with stormwater contamination. He added, "Using SAR is a way to decide where to sample most effectively."



The Los Angeles River flows low in the dry season, which includes spring and summer. (Courtesy ruggbear/Flickr)

City slicker

Holt also knew SAR had its limitations, so he contacted Gierach, who specializes in ocean color sensors, such as the Moderate-Resolution Imaging Spectroradiometer (MODIS) on NASA's Aqua satellite. By incorporating another characteristic of stormwater runoff—the sediment discharge—could more insights be made on stormwater runoff in southern California?

Cloud cover during or after storms limits MODIS, and with SAR data being sporadic, only seven rainstorms matched up MODIS and SAR imagery, offering the researchers a comparison of how each instrument sees the coastal ocean.

MODIS detects turbidity, or the water's cloudiness. "With these major precipitation events, a lot of material is being dumped into the ocean that would be characteristically different than the surrounding waters," Gierach said. "We're not specifically teasing out this or that pollutant. We're just saying we know that this water mass is entirely different." The MODIS sediment plumes were considerably larger than the SAR surface slick plumes. The signature from SAR images is generally smaller in size and is observed for a shorter period since the surface plume eventually mixes and spreads out into the ocean. Though trash and debris may still be present, diluted concentrations are less able to dampen ocean waves. Since MODIS picks up larger plumes, anyone interested in offshore testing can target a larger contaminated area.

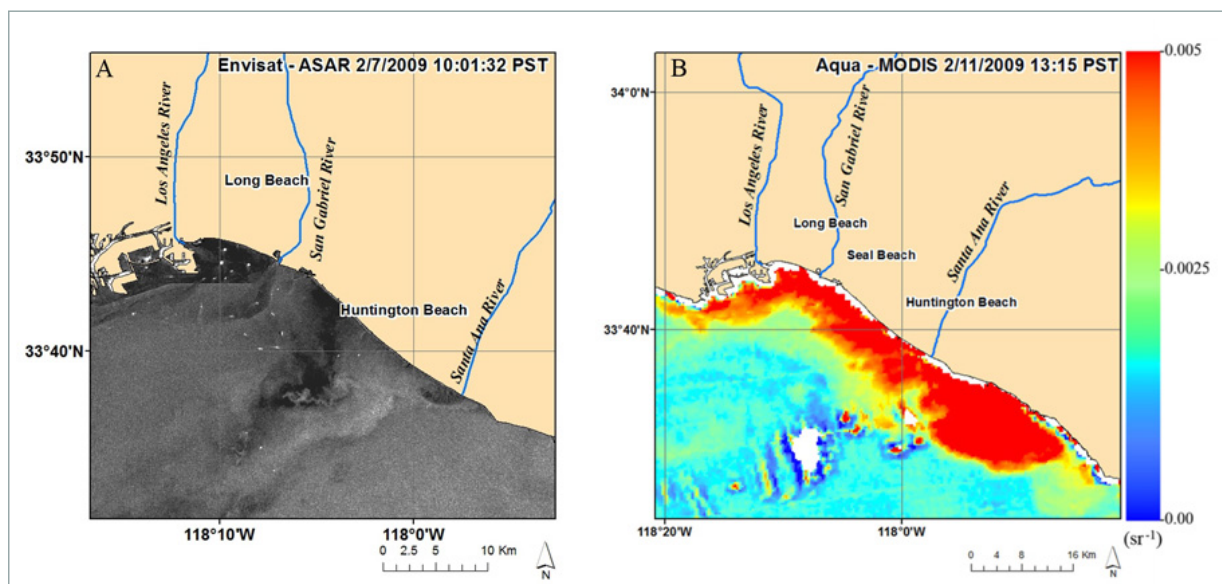
On the other hand, SAR snaps images at night and during a rainstorm, when considerable cloud coverage blocks the MODIS sensor, allowing SAR to always be the first to detect stormwater runoff plumes.

SAR, coupled with MODIS, fill each other's gaps. "Clearly there are some limitations," Gierach said. But knowing the caveats associated with each instrument should not be a deterrent in using them. "There are limitations, but the

information you can get by a combination of remote sensing sensors is still so key that I think it outweighs the limitations," she added.

As for the LA River, reducing the contaminants from industrial sites, catching larger items like branches and plastic cups in catchment areas, could help abate toxic and harmful matter from entering the ocean. Exposing more soil to retain rain is another solution, but this option has to be weighed carefully since a major city stands in the river's way. Recently, an agreement between LA and the federal government hopes to revitalize the LA River with a \$1.3 billion restoration effort, covering an 18-kilometer (11-mile) stretch, where concrete encasements will be removed to green up the river and create an urban oasis with a bike path, parks, and business.

Still, ocean-borne illnesses, according to LA County health officials, cause \$20 million dollars annually in health-related costs. In the end, whether the goal is healthier beaches, improving public health, successful wastewater diversions, or ocean monitoring, Gierach envisions more pairings between specific agencies, their needs, and NASA data. "The true merit of remote sensing should be advocated more broadly to engage specific agencies," Gierach said.



These two maps compare the same stormwater plume as observed from two different satellite sensors. Synthetic Aperture Radar (SAR) on the left was taken on February 07, 2009 and the NASA Moderate Resolution Imaging Spectroradiometer (MODIS) on the right was taken on February 11, 2009. The white areas on the MODIS image represent cloud cover and land surface interference near the coast. In the SAR image (A) darker areas capture a smoother surface slick, or dampened ocean wave height. In the MODIS (B) image, the warmer (red) the reflectance signal, the more turbid, or cloudy, the ocean, while cooler (blue) colors signify clearer waters. (Courtesy B. Holt et al., 2017, *Marine Pollution Bulletin*)

For more information

[NASA Alaska Satellite Facility \(ASF\) Distributed Active Archive Center \(DAAC\)](#)

[NASA Ocean Biology DAAC \(OB.DAAC\)](#)

[Japan Aerospace Exploration Agency \(JAXA\) Advanced Land Observing Satellite \(ALOS\)](#)

[JAXA Phased Array type L-Band Synthetic Aperture Radar \(PALSAR\)](#)

[NASA Moderate Resolution Imaging Spectroradiometer \(MODIS\)](#)

[Synthetic Aperture Radar](#)

[Heal the Bay](#)

References

Gierach, M., B. Holt, R. Trinh., B. Pan, and C. Rains. 2016. Satellite detection of wastewater diversion plumes in Southern California. *Estuarine, Coastal and Shelf Science*. doi:10.1016/j.ecss.2016.10.012 [↗](#).

Holt, B., R. Trinh, and M. M. Gierach. 2017. Stormwater runoff plumes in the Southern California Bight: A comparison study with SAR and MODIS imagery. *Marine Pollution Bulletin* 118: 141-154. doi:10.1016/j.marpolbul.2017.02.040 [↗](#).

NASA Alaska Satellite Facility Distributed Active Archive Center (ASF DAAC). 2017. ALOS PALSAR data. Copyrighted by JAXA, METI. Fairbanks, AK, USA: NASA ASF DAAC. <https://www.asf.alaska.edu/sar-data/palsar/about-palsar> [↗](#).

NASA Alaska Satellite Facility Distributed Active Archive Center (ASF DAAC). 2017. Uninhabited Aerial Vehicle Synthetic Aperture Radar (UAVSAR) data. Fairbanks, AK, USA. <https://www.asf.alaska.edu/sar-data/uavsar/> [↗](#)

NASA Goddard Space Flight Center, Ocean Ecology Laboratory, Ocean Biology Processing Group. 2017. Moderate-resolution Imaging Spectroradiometer (MODIS) Aqua Ocean Color Data. NASA Ocean Biology Distributed Active Archive Center (OB.DAAC), Greenbelt, MD, USA. <https://oceancolor.gsfc.nasa.gov/data/10.5067/AQUA/MODIS/L2/OC/2018/> [↗](#)

About the remote sensing data			
Satellites	Aqua	Japan Aerospace Exploration Agency (JAXA) Advanced Land Observing Satellite (ALOS)	
Platform			NASA Gulfstream III (G-III) Research Testbed Aircraft
Sensors	Moderate Resolution Imaging Spectroradiometer (MODIS)	Phased Array type L-Band Synthetic Aperture Radar (PALSAR)	Uninhabited Aerial Vehicle Synthetic Aperture Radar (UAVSAR)
Data sets	Level-1 radiance data ↗	ALOS PALSAR L1.1 ↗	UAVSAR ↗
Resolution	555 nanometers	100 meters	7 meters
Parameters	Ocean color/reflectance	Reflectance	Reflectance
DAACs	NASA Ocean Biology Distributed Active Archive Center (OB.DAAC)	NASA Alaska Satellite Facility (ASF) Distributed Active Archive Center (DAAC)	NASA ASF DAAC

When the big picture is not enough



A researcher pushes the limits of radar data to monitor small rice fields in the Philippines.

By Natasha Vizcarra

Every twelve days, agricultural engineer Ritche Nuevo took his meter stick, caliper, and a notebook to a small rice field close to his home. Nuevo lives and works in the coastal town of Argao, on the Philippine island of Cebu. When he was not teaching or spending time with his wife and kids, he was often at the rice field measuring growing rice plants. He kept a list of days to visit the flooded paddies that coincided with the European Space Agency's Sentinel-1 satellite flying over the archipelago, 692 kilometers (430 miles) above him.

- [About the data](#)
- [About ASF DAAC](#)

Ranging from school bus-sized to small as a Rubik's Cube, satellites orbit Earth several times a day. Whatever the size, most satellites measure continents and large countries best, particularly because they are so far away from what they are measuring. In the last few years, however, some satellites have been equipped with better sensors that can see Earth's surface at very high resolution, or in more detail. Launched in 2014, Sentinel-1 was one of those satellites.

"I was intrigued by the possibility of using Sentinel-1 data to monitor small-scale rice farms, which are common here in the Philippines," Nuevo said.

Nuevo wanted to find a way to track rice growth using Sentinel-1 to help small-scale rice farmers and agencies assisting farmers quickly estimate crop damage from droughts and strong typhoons. Storms blow through the Philippine archipelago from June to October, sometimes destroying crops with relentless rains and gale-force winds. Timely assessments of rice damage are crucial in rice-dependent countries like the Philippines, which would need to quickly import the crop to prevent an acute national shortage.



Ritche Nuevo measures a rice plant at a field in Argao, Philippines. (Courtesy R. U. Nuevo)

How small is small?

Filipinos eat rice for breakfast, lunch, and dinner. Its flour form is a common ingredient in many beloved desserts, like puffy, steamed rice cakes called *puto* and savory-sweet pastries called *bibingka*. Unlike the sprawling, industrial fields of wheat and corn in the Northern Hemisphere, about 80 percent of the world's rice is grown by farmers in small fields, in low-income and developing countries like the Philippines.

If you fly a camera drone over the Philippine countryside, you will see smallish blocks of rice fields peppering the margins of rural towns and small cities. They rarely occur as large, contiguous crop fields. An individual farmer in the Philippines generally operates 2 hectares (5 acres), slightly smaller than the average 3-hectare (7-acre) Southeast Asian rice farm. By comparison, the average agricultural farm size in the United States is 180 hectares (445 acres).

That was why Nuevo homed in on Sentinel-1. The researcher previously came across studies about satellite sensors able to recognize 3-by-3-kilometer (5-by-5-mile) rice fields, equivalent to 300 hectares or 740 acres. "That's just too large for typical applications in the Philippines," Nuevo said. "It wouldn't be able to pick up the differences between one land use and another." Sentinel-1 data, on the other hand, covered a 10-by-10-meter (33-by-33-foot), equivalent to 0.01 hectares or 0.25 acres area, and—unlike other satellite sensors—the Sentinel-1 radar could collect data in the rainy tropics. "The radar can penetrate clouds," Nuevo said. "So, our monsoon weather was not a problem."



A Google Earth image shows the study site, outlined in yellow, in the middle of a field of other rice fields, all separately owned and managed by different farmers. (Courtesy Google Earth)

When calamity strikes

Rice is grown and harvested twice a year in the Philippines. At the beginning of every planting season, fields go through a process called puddling, where after flooding the land is plowed to mix and level the soil. Rice seedlings are then transplanted to the prepared field. It takes around three to four months for rice plants to mature. At harvest time, farmers collect the plants and then manually or mechanically thresh them to separate the grains from the straw. Farmers dry the grains and typically sell to millers. At the mills, machines hull and polish the grains until the rice germ and bran layer come off. Rice millers and traders sell processed rice as white rice and unpolished rice as brown rice.

The Philippines' National Food Authority (NFA) maintains the country's buffer stock, a system that buys and stores rice during good harvest seasons to prevent prices from falling below a price level that might hurt the industry, and releases the stocks during seasons of bad harvests to prevent rice prices from rising beyond consumers' reach. When inventories fall below the NFA's 90-day buffer stock, the country imports rice.

Because the country is smack-dab in the Pacific's typhoon belt, it has not been able to produce enough rice to export. Instead, it buys rice from neighboring countries—such as Thailand and Vietnam—that are fairly sheltered from storms that develop in the Pacific.

Strong typhoons can cause rice prices in the Philippines to increase, based solely on speculation. Anticipating a shortage and a rise in demand, farmers sell grains to millers at higher prices, and millers hike up bulk prices when selling to traders. A drastic price increase can trigger the NFA to release rice from the buffer stock to stabilize prices. That is why it is crucial to have actual data on crop damage. In rice-producing provinces, local officials generally need to survey damage on foot. "Immediate, on-the-ground assessment is often a challenge because of floods, road obstructions, and infrastructure damage," said Alice Laborte, a researcher at the International Rice

Research Institute in Laguna, Philippines. “Remote sensing can play a role in rapid, cost-effective, and—most importantly—objective assessment of damage over a wide area.”



A farmer harvests rice at a field in Laguna, Philippines. (Courtesy International Rice Research Institute)

Seeking a unique signature

In Argao, Nuevo first needed to test the theory that Sentinel-1 data can be used to differentiate rice fields from other types of surfaces. He found a 6,320-square meter (20,730-square foot), or 0.63-hectare (1.56-acre) rice field in the beginning of its growing season, conveniently near his home and near the university where he worked. The field sat in the middle of other small rice fields, all separately owned and managed by different farmers.

Nuevo collected field data from seeding in October 2016 to its harvest in February 2017, measuring a set of the plants’ physical properties that signal growth, such as height and number of stems that sprouted leaves and grains. The field sampling points, marked by bamboo stakes, were 10 to 30 meters (33 to 98 feet) apart, approximating the Sentinel-1 10-by-10-meter (33-by-33-foot) pixel resolution. He also selected grass covered ground, an area with trees, and an inland pond to represent ground, trees, and water surfaces to compare with the rice field.

He then acquired Level-1 Ground Range Detected (GRD) Sentinel-1 data from the NASA Alaska Satellite Facility Distributed Active Archive Center. The Sentinel-1 C-Band Synthetic Aperture Radar (SAR) sends radar pulses to Earth, which bounce off different surfaces and are reflected, or backscattered, to the sensor. Nuevo plotted out a whole planting season’s worth of backscattered signals from his study site and the nearby sample sites for trees, water, and ground, and found the unique pattern for rice.

Backscatter dropped during the flooding and puddling of the rice field at the beginning of the planting season, whereas signals from the other surface types generally remained the same. This is because radar scatters in a forward motion when it bounces off a flat surface like a flooded rice field, resulting in low backscatter readings. As the crops grew and water levels in the paddies fell, backscatter from the rice field increased while backscatter from the other surfaces remained the same.

Nuevo was elated. “Many studies have successfully identified and mapped rice canopies using C-Band SAR, but none have attempted to apply it at the scale of a single pixel,” Nuevo said. Would the data prove useful in

detecting the actual growth of the plants throughout a growing season? And would it detect the lack of growth that might happen with storm damage?



Rice seedlings are transplanted to a flooded and plowed rice field. (Courtesy International Rice Research Institute)

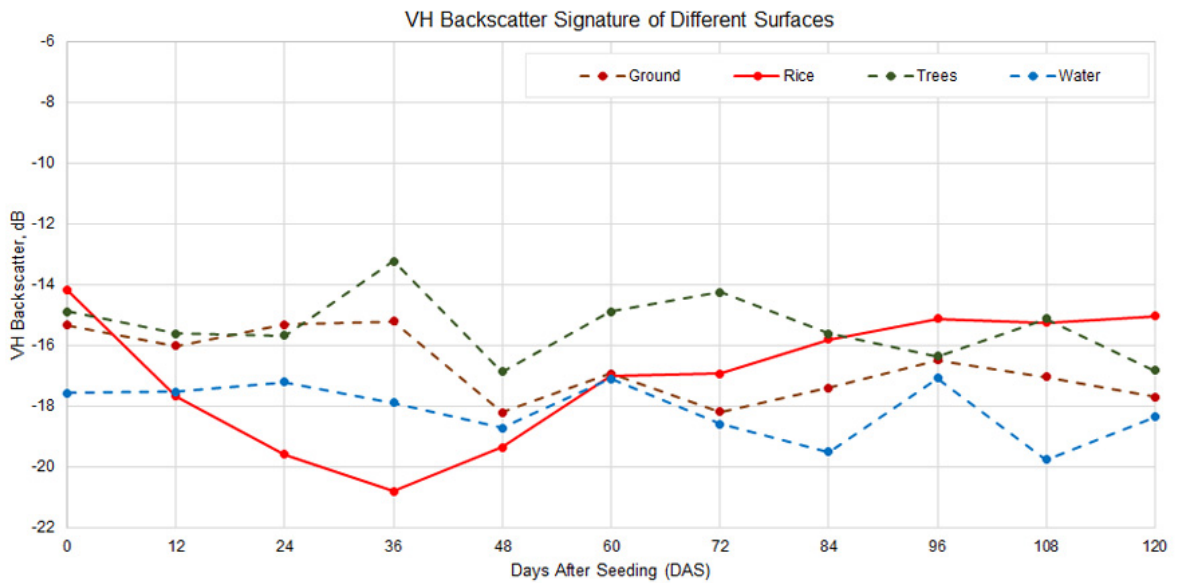
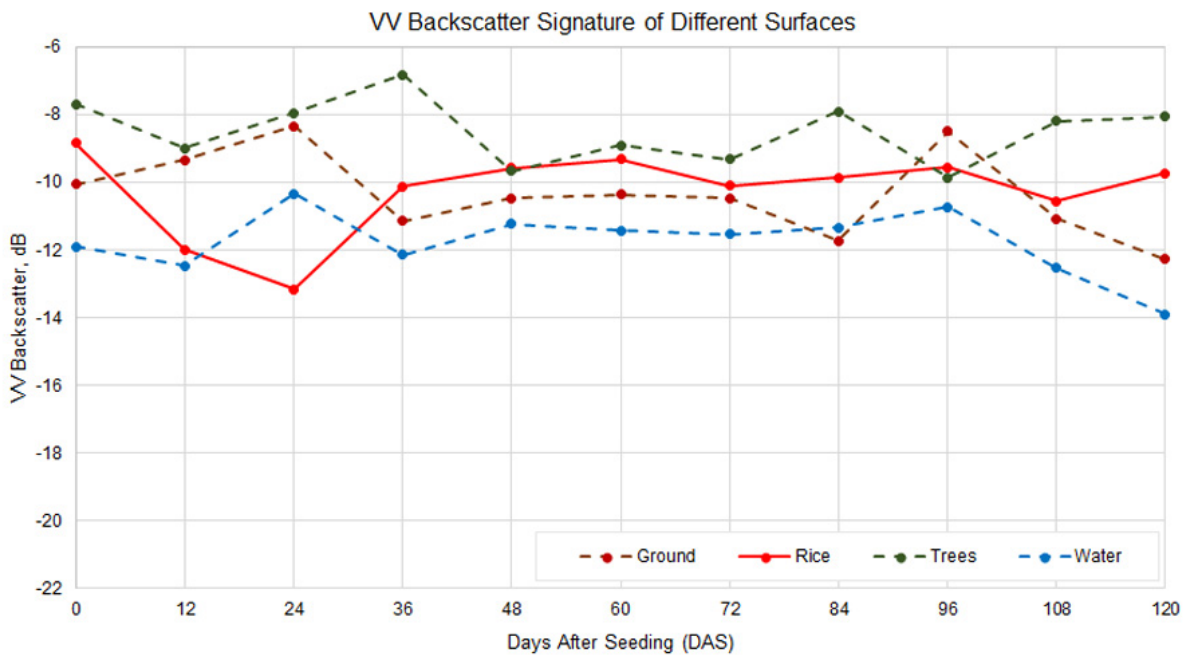
Better backscatter

Nuevo ran an analysis of the field and satellite data and found that the radar's Vertical-Horizontal or VH, backscatter correlated well with changes in the plants' height and diameter, meaning the signals could sense subtle changes in these two parameters throughout the growing season. C-Band SAR sends and receives two kinds of signals: VH pulses are sent out vertically and received horizontally, and Vertical-Vertical (VV) pulses are sent out vertically and are received vertically by the satellite sensor.

Unfortunately, Nuevo's finding contradicted other studies that suggest VV signals can see rice growth better. "Rice plants are generally upright so VV almost always gets a strong backscatter," Nuevo said. "Although VH backscatter from the rice plants is not as strong, it correlates well with plant height. So, clearly, this is an area for further studies."

One final finding posed an exciting possibility. "I noticed that adjacent Sentinel-1 pixels can be very different from each other," he said. Nuevo's sampling points were 10 to 30 meters (33 to 98 feet) apart. His analysis showed that his sampling points—all in one row and in the same rice field—produced slightly different backscatter readings from each other.

Nuevo suspects that Sentinel-1 is capable of sensing small differences in vegetation between points that are just a pixel apart. "Such sensitivity has a huge potential for future monitoring studies in rice," he said. "This would be great for small village applications. Though remotely-sensed data get us a big picture, you can still get a smaller picture out of that bigger one."



These graphs show Vertical-Vertical (VV) and Vertical-Horizontal (VH) backscatter in decibels (dB) for rice and other reference surfaces during the cropping period. Brown dashed lines represent the ground, blue dashed lines water, green dashed lines trees, and solid red lines represent rice. The horizontal axes shows number of days after seeding (DAS). (Courtesy R. Nuevo)

For more information

[NASA Alaska Satellite Facility \(ASF\) Distributed Active Archive Center \(DAAC\)](#)

[Sentinel-1](#)


References

NASA Alaska Satellite Facility Distributed Active Archive Center. 2018. SENTINEL-1A_DUAL_POL_GRD_FULL_RES. Fairbanks, AK, USA: NASA ASF DAAC. <https://www.asf.alaska.edu/sentinel/data>

Nuevo, R. U., R. B. Saludes, M. A. Dorado, and N. C. Bantayan. 2017. Monitoring of rice in small paddy fields using multi-temporal Sentinel-1 data. Paper presented at the 38th Asian Conference on Remote Sensing, New Delhi,

India, October 2017.

Royandoyan, O. M. 2015. Small farms and Philippine agriculture. Paper presented at the Conference on Contested Access to Land, Quezon City, Philippines, February 2015.

About the remote sensing data	
Satellite	Sentinel-1
Sensor	C-Band Synthetic Aperture Radar
Data set	SENTINEL-1A_DUAL_POL_GRD_FULL_RES 
Resolution	10 x 10 meter
Parameter	Reflectance
DAAC	NASA Alaska Satellite Facility (ASF) Distributed Active Archive Center (DAAC)